

BRITISH GEOLOGICAL SURVEY

Lerwick Observatory

Monthly Magnetic Bulletin

**September
2019**

19/09/LE



SHETLAND
ISLANDS



**British
Geological Survey**

NATURAL ENVIRONMENT RESEARCH COUNCIL

LERWICK OBSERVATORY MAGNETIC DATA

1. Introduction

Lerwick observatory is one of three geomagnetic observatories in the UK operated and maintained by the British Geological Survey (BGS).

This bulletin is published to provide rapid access to the provisional geomagnetic observatory results. The information is freely available for personal, academic, educational and non-commercial research or use. Magnetic observatory data are presented as a series of plots of one-minute, hourly and daily values, followed by tabulations of monthly values, reports of rapid variations and geomagnetic activity indices. The operation of the observatory and presentation of data are described in the rest of this section.

Enquiries about the data should be addressed to:

Geomagnetism Team
British Geological Survey
Lyell Centre, Heriot Watt University
Research Avenue South
Edinburgh EH9 3LA
Scotland, UK

Tel: +44 (0) 131 667 1000
E-mail: enquiries@bgs.ac.uk
Internet: www.geomag.bgs.ac.uk

2. Position

The observatory is situated on a ridge of high ground about 2.5 km to the SW of the port of Lerwick in Shetland. The observatory co-ordinates are:

Geographic: 60°08'16.8"N 358°49'01.2"E
Geomagnetic: 61°45'00"N 088°40'02"E
Height above mean sea level: 85 m

The geographical coordinates are measured by a handheld GPS device, which uses WGS84 as the reference coordinate system. The height above MSL is determined from the best available contour maps. The geomagnetic co-ordinates are approximations, calculated using the 12th generation International Geomagnetic Reference Field (IGRF) at epoch 2019.5. On-line access to models (including IGRF), charts and navigational data are available at www.geomag.bgs.ac.uk/data_service/models_compass/home

3. The Observatory Operation

3.1 GDAS

The observatory operates under the control of the Geomagnetic Data Acquisition System (GDAS), which was developed by BGS staff, installed in 2002, and became fully operational in January 2003. The data acquisition software, running on QNX operated computers, controls the data logging and the communications.

There are two sets of sensors used for making magnetic measurements. A tri-axial linear-core fluxgate magnetometer, manufactured by the Danish Meteorological Institute, is used to measure the variations in the horizontal (H) and vertical (Z) components of the field. The third sensor is oriented perpendicular to these, and measures variations, which are proportional to the changes in declination (D). Measurements are made at a rate of 1 Hz.

In addition to the fluxgate sensors there is a proton precession magnetometer (PPM) making measurements of the absolute total field intensity (F) at a rate of 0.1Hz.

The raw unfiltered data are retrieved automatically via Internet connections to the BGS office in Edinburgh in near real-time. The fluxgate data are filtered to produce one-minute values using a 61-point cosine filter and the total field intensity samples are filtered using a 7-point cosine filter. The one-minute values provide input for various data products, available on-line at www.geomag.bgs.ac.uk/data_service/home

3.2 Back-up Systems

There are two other fully independent identical systems, GDAS 2 and GDAS 3, operating at the observatory. The data from these are also processed in near real-time and used for quality control purposes. They are also used to fill any gaps or replace any corrupt values in the primary system, GDAS 1.

3.3 Absolute Observations

The GDAS fluxgate magnetometers accurately measure variations in the components of the geomagnetic field, but not the absolute magnitudes. Two sets of absolute measurements of the field are made manually once per week. A fluxgate sensor mounted on a theodolite is used to determine D and inclination (I); the GDAS PPM measurements, with a site difference correction applied, are used for F .

The absolute observations are used in conjunction with the GDAS variometer measurements to produce a continuous record of the absolute values of the geomagnetic field elements as if they had been measured at the observatory reference pillar.

4. Observatory Results

The data presented in the bulletin are in the form of plots and tabulations described in the following sections.

4.1 Absolute Observations

The absolute observation measurements made during the month are tabulated. Also included are the corresponding baseline values, which are the differences between the absolute measurements and the variometer measurements of D , H and Z (in the sense absolute–variometer). These are also plotted (markers) along with the derived preliminary daily baseline values (line) throughout the year. Daily mean differences between the measured absolute F and the F computed from the baseline corrected H and Z values are plotted in the fourth panel (in the sense measured–derived). The bottom panel shows the daily mean temperature in the fluxgate chamber.

4.2 Summary magnetograms

Small-scale magnetograms are plotted which allow the month's data to be viewed at a glance. They are plotted 16 days to a page and show the one-minute variations in D , H and Z . The scales are shown on the right-hand side of the page. On disturbed days the scales are multiplied by a factor, which is indicated above the panel for that day. The variations are centred on the monthly mean value, shown on the left side of the page.

4.3 Magnetograms

The daily magnetograms are plotted using one-minute values of D , H and Z from the fluxgate sensors, with any gaps filled using back-up data. The magnetograms are plotted to a variable scale; scale bars are shown to the right of each plot. The absolute level (the monthly mean value) is indicated on the left side of the plots.

4.4 Hourly Mean Value Plots

Hourly mean values of D , H and Z for the past 12 months are plotted in 27-day segments corresponding to the Bartels solar rotation number. Magnetic disturbances associated with active regions and/or coronal holes on the Sun may recur after 27 days: the same is true for geomagnetically quiet intervals. Plotting the data in this way highlights this recurrence. Diurnal variations are

also clear in these plots and the amplitude changes throughout the year highlight the seasonal changes. Longer term secular variation is also illustrated.

Full lists of the UK observatory hourly mean values from 1983 to the present day are available at www.geomag.bgs.ac.uk/data_service/data/obs_data/hourly_means

4.5 Daily and Monthly Mean Values

Daily mean values of D , H , Z and F are plotted throughout the year. In addition, a table of monthly mean values of all the geomagnetic elements is provided. These values depend on accurate specification of the fluxgate sensor baselines. It is anticipated that these provisional values will not be altered by more than a few nT or tenths of arcminutes before being made definitive at the end of the year.

4.6 Rapid Variations

Charged particles stream from the Sun in the solar wind. The solar wind interacts with the geomagnetic field to create a cavity, the magnetosphere, in which the field is confined. When a region of enhanced velocity and/or density in the solar wind arrives at the dayside boundary of the magnetosphere (at about 10 earth radii) the boundary is pushed towards the Earth. Currents set up on the boundary of the magnetosphere can cause an abrupt change in the geomagnetic field measured on the ground and this is recorded on observatory magnetograms as a sudden impulse (*si*). If, following an *si*, there is a change in the rhythm of activity, the *si* is termed a storm sudden commencement (*ssc*). A classical magnetic storm exhibiting initial, main and recovery phases (shown by, for instance, the *Dst* ring current index) can often occur after a *ssc*, in which case the start of the storm is taken as the time of the *ssc*.

Solar flares, seen at optical wavelengths as a sudden brightening of a small region of the Sun's surface, are also responsible for increased X-ray emissions. These X-rays cause increased ionisation in the ionosphere, which leads to absorption of short-wave radio signals. A solar flare effect (*sfe*), or "crochet", may be observed on a magnetogram during geomagnetically quiet times. It is a relatively short-term change (tens of minutes) to the normal diurnal variation and can vary in size (tens of nT) depending on local time (LT), geomagnetic latitude and solar zenith angle.

4.7 Local geomagnetic activity indices

The Observatory K index. This summarises geomagnetic activity at an observatory by assigning

a code, an integer in the range 0 to 9, to each 3-hour Universal Time (UT) interval. The index for each 3-hour UT interval is determined from the maximum range in H or D (scaled in nT), with allowance made for the regular (undisturbed) diurnal variation. The conversion from range to an index value is made using a quasi-logarithmic scale, with the scale values dependent on the geomagnetic latitude of the observatory. The lower bounds (in nT) for the classification of each period at Lerwick are:

| | | | | | | | | | |
|---|----|----|----|----|-----|-----|-----|-----|------|
| 0 | 1 | 2 | 3 | 4 | 5 | 6 | 7 | 8 | 9 |
| 0 | 10 | 20 | 40 | 80 | 140 | 240 | 400 | 660 | 1000 |

The K index retains the LT and seasonal dependence of activity associated with the position of the observatory. The 3-hourly K indices for the month are tabulated and also plotted as a histogram. All UK observatory K indices are available at www.geomag.bgs.ac.uk/data_service/data/magnetic_indices/k_indices

4.8 Global geomagnetic activity indices

The aa index. A number of 3-hour geomagnetic indices are computed by combining K indices from networks of observatories to characterise global activity levels and to eliminate LT and seasonal effects. The simplest of these is the aa index, computed using the K indices from two approximately antipodal observatories: Hartland in the UK and Canberra in Australia. The aa index is calculated from linearisations of the Hartland and Canberra K indices, and has units of nT. The 3-hourly aa indices are tabulated along with the daily mean value of aa (denoted Aa), the mean values of aa for the intervals 00-12UT (Aa_{am}) and 12-24UT (Aa_{pm}) and the monthly mean value. The 3-hourly aa indices for the month are also plotted as a histogram.

Although the aa index is based on data from only two observatories, provided averages over 12 hours or longer are used, the index is strongly correlated with the ap and am indices, which are derived using data from more extensive observatory networks.

The aa indices listed in this bulletin are available at www.geomag.bgs.ac.uk/data_service/data/magnetic_indices/aaindex as well as the full data set from 1868.

Definitive aa are published by the International Service for Geomagnetic Indices, EOST, 5 rue René Descartes, 67084 Strasbourg Cedex, France.

5. Conditions of Use

The data presented in this bulletin are provided for personal, academic, educational, non-commercial research or other non-commercial use and are not for sale or distribution to third parties without written permission from BGS.

Reproduction of any part of this bulletin should be accompanied by the statement: 'Reproduced with the permission of the British Geological Survey ©NERC. All rights Reserved'. Publications making use of the data should include an acknowledgment statement of the form: 'The results presented in this paper rely on the data collected at Lerwick magnetic observatory, operated by the British Geological Survey.'

Commercial users can contact the geomagnetism team for information on the range of applications and services offered. Full contact details are available at www.geomag.bgs.ac.uk/contactus/staff

**This product includes mapping data licensed from Ordnance Survey with the permission of HMSO © Crown copyright. All rights reserved.
Licence Number: 100017897/2019**

LERWICK OBSERVATORY

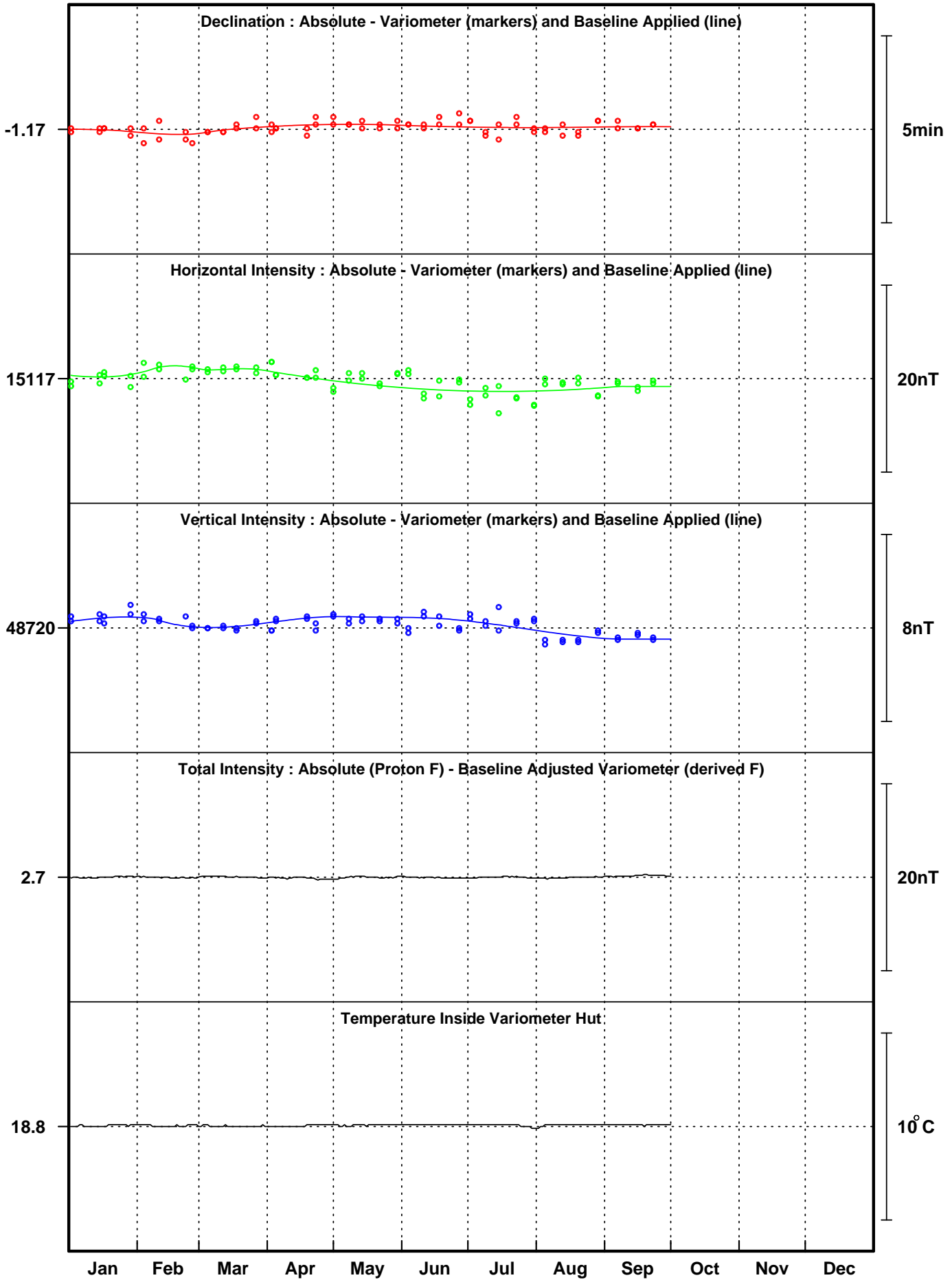
ABSOLUTE OBSERVATIONS

| Date | Day Number | Declination | | | Inclination | | Total Field | | Horizontal Intensity | | Vertical Intensity | | Observer |
|-----------|------------|-------------|--------------|--------------|-------------|--------------|----------------------|-------------------------|----------------------|---------------|--------------------|---------------|----------|
| | | Time (UT) | Absolute (°) | Baseline (°) | Time (UT) | Absolute (°) | Site difference (nT) | Absolute corrected (nT) | Absolute (nT) | Baseline (nT) | Absolute (nT) | Baseline (nT) | |
| 06-Sep-19 | 249 | 06:08 | -0.8450 | -1.1617 | 06:22 | 72.8194 | -2.7 | 51005.4 | 15066.2 | 15116.8 | 48729.5 | 48719.5 | NL |
| 06-Sep-19 | 249 | 06:32 | -0.8217 | -1.1650 | 06:43 | 72.8151 | -2.7 | 51012.4 | 15071.9 | 15117.0 | 48735.1 | 48719.4 | NL |
| 15-Sep-19 | 258 | 15:38 | -0.9271 | -1.1650 | 15:55 | 72.8188 | -2.7 | 51041.4 | 15077.3 | 15116.0 | 48763.7 | 48719.7 | DOC |
| 15-Sep-19 | 258 | 16:04 | -0.9129 | -1.1650 | 16:16 | 72.8206 | -2.7 | 51045.4 | 15077.0 | 15116.4 | 48768.0 | 48719.6 | DOC |
| 22-Sep-19 | 265 | 15:19 | -0.9178 | -1.1633 | 15:33 | 72.8272 | -2.7 | 51029.3 | 15066.7 | 15117.1 | 48754.3 | 48719.4 | AM |
| 22-Sep-19 | 265 | 15:46 | -0.9001 | -1.1633 | 16:00 | 72.8255 | -2.7 | 51030.0 | 15068.3 | 15116.8 | 48754.6 | 48719.5 | AM |
| | | | | | | | | | | | | | |
| | | | | | | | | | | | | | |

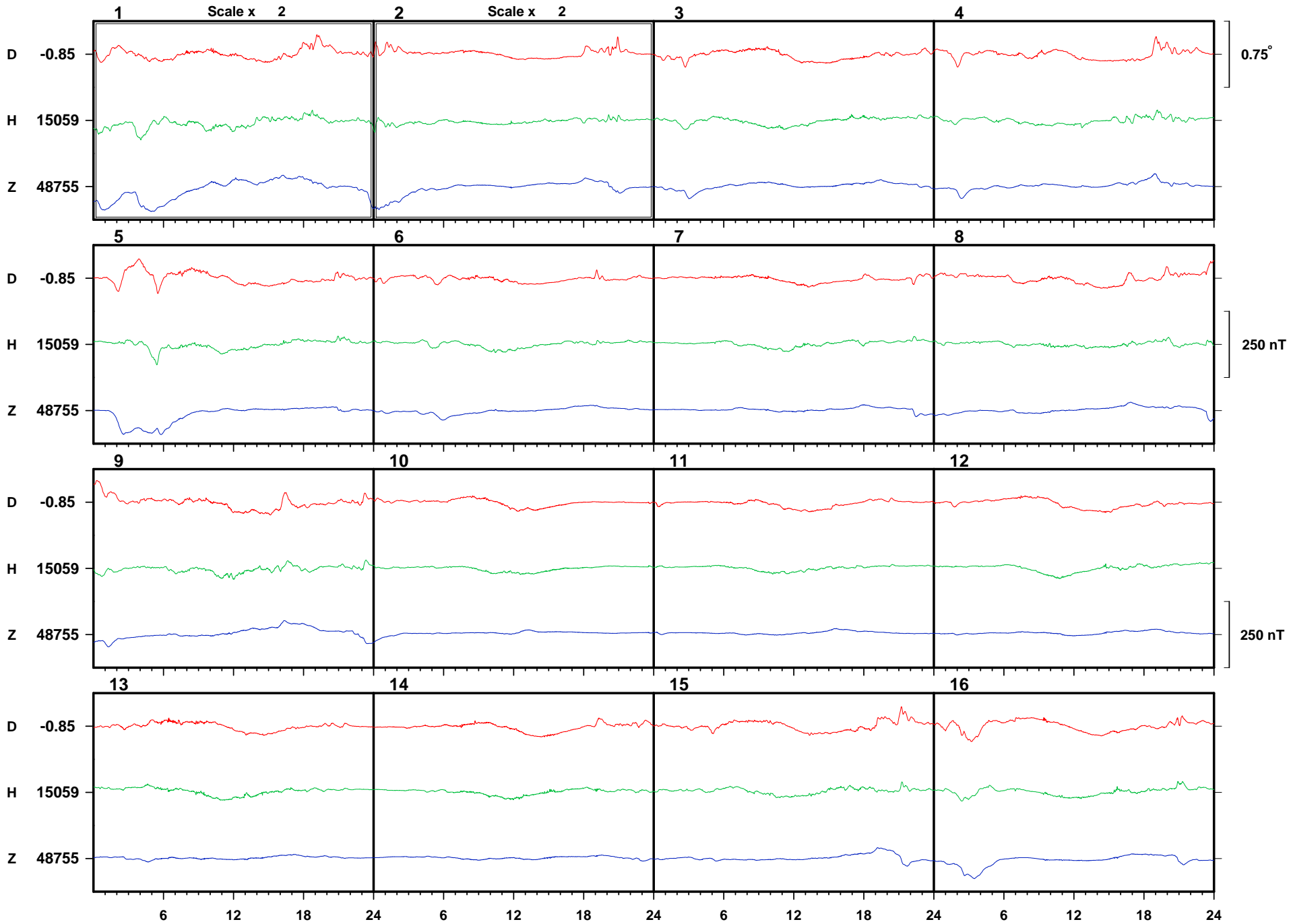
Note:

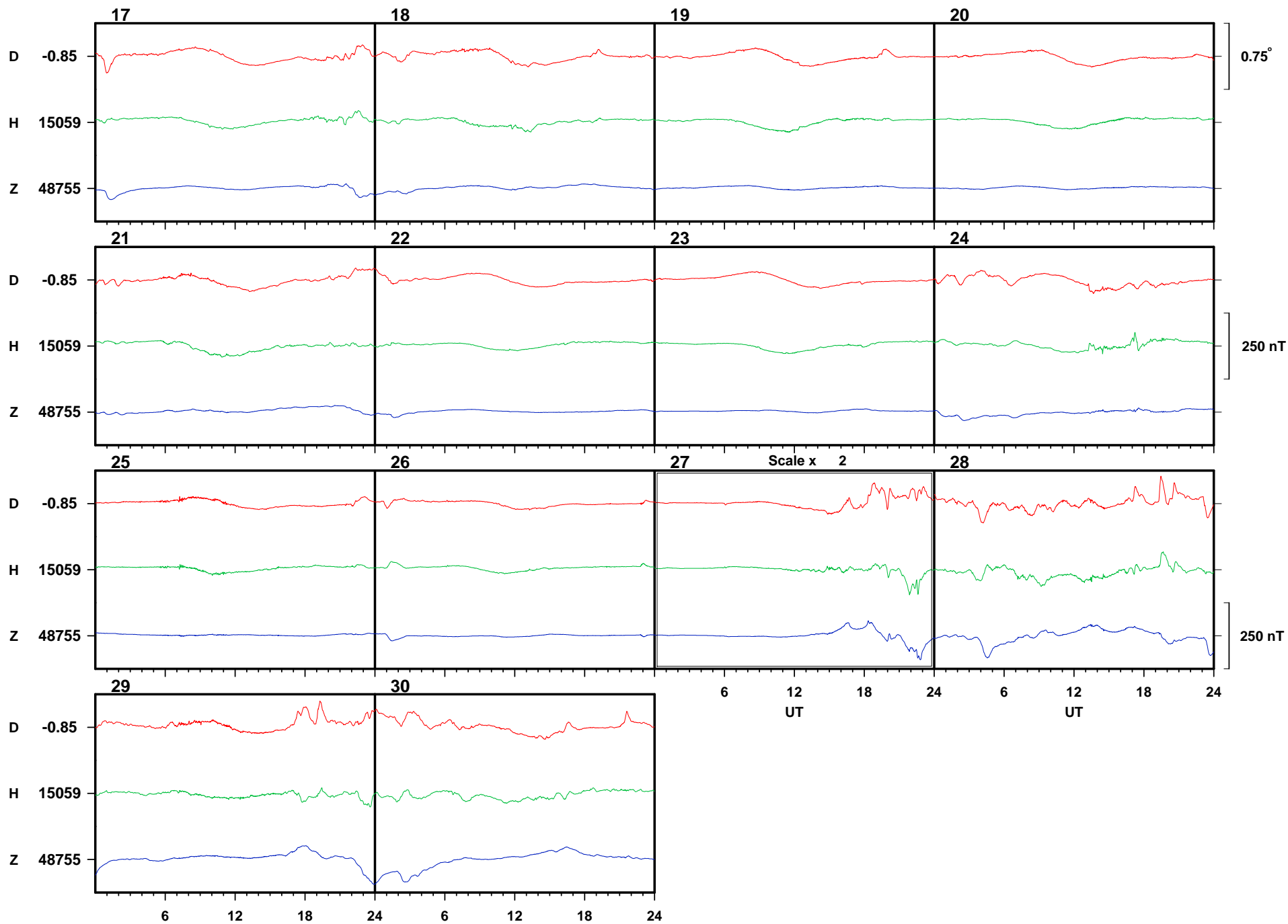
1: 999.9999 and 99999.9 denote a flagged value

Lerwick 2019



Lerwick September 2019





Lerwick

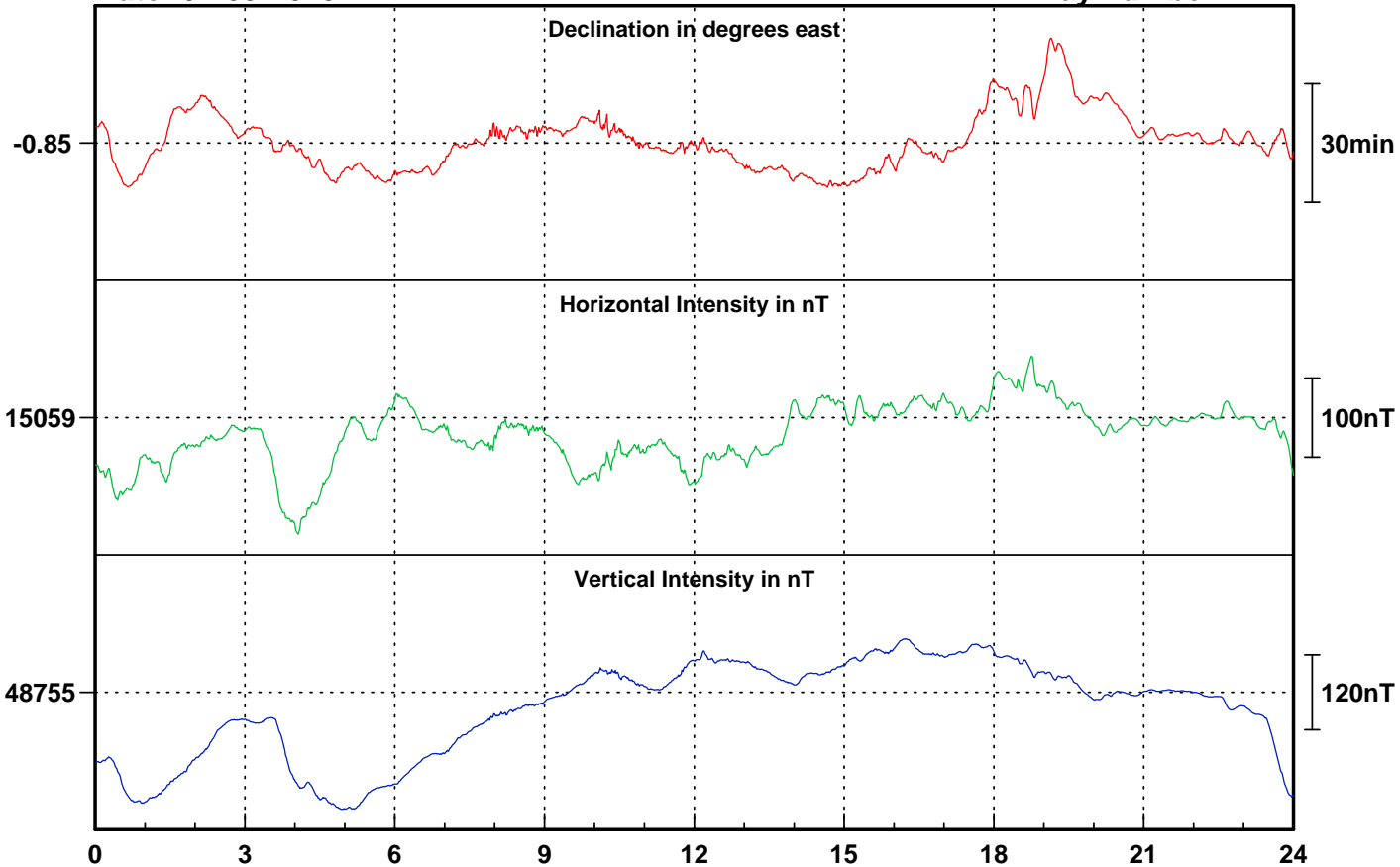
September

2019

Date: 01-09-2019

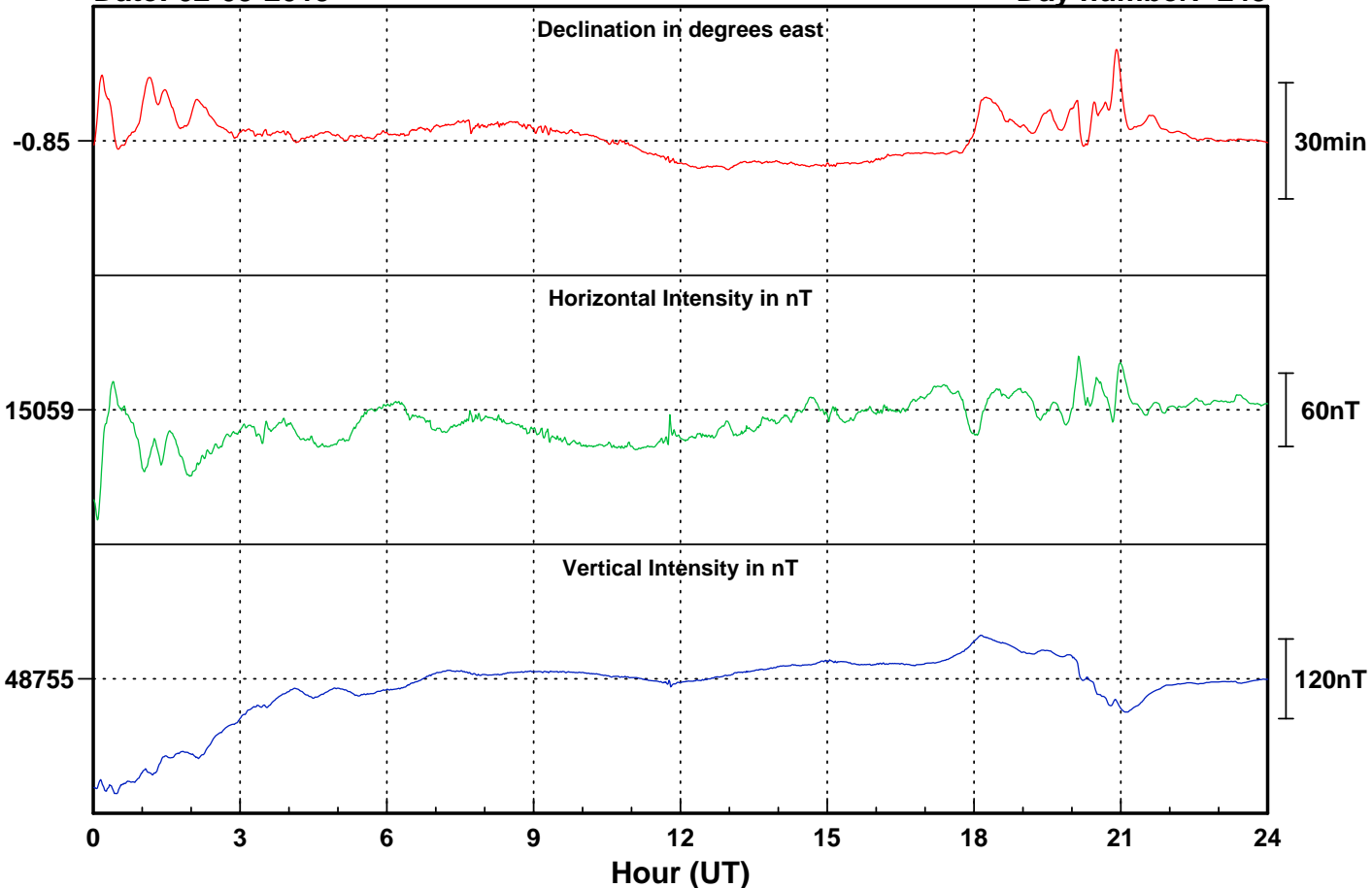
Lerwick

Day number: 244



Date: 02-09-2019

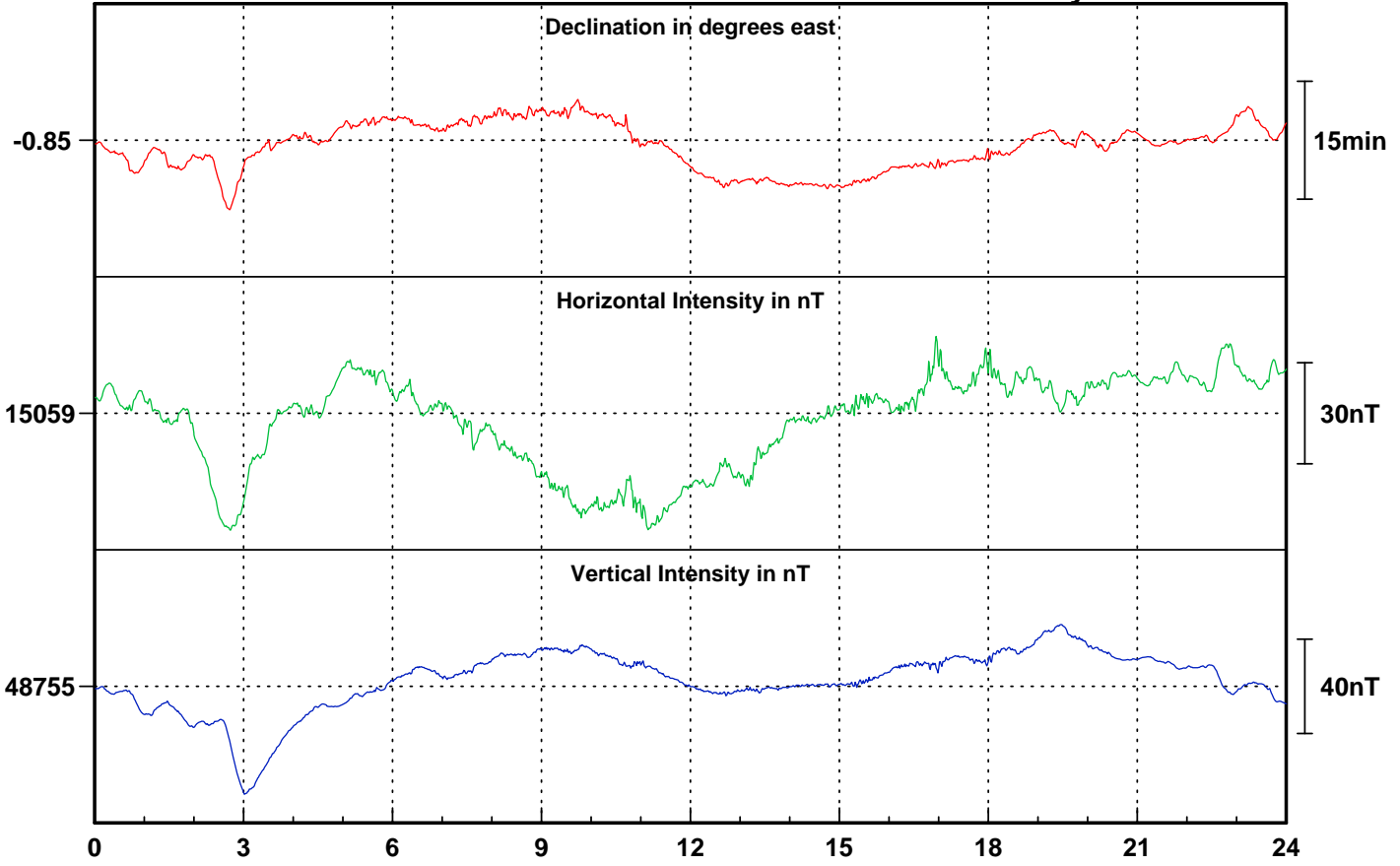
Day number: 245



Date: 03-09-2019

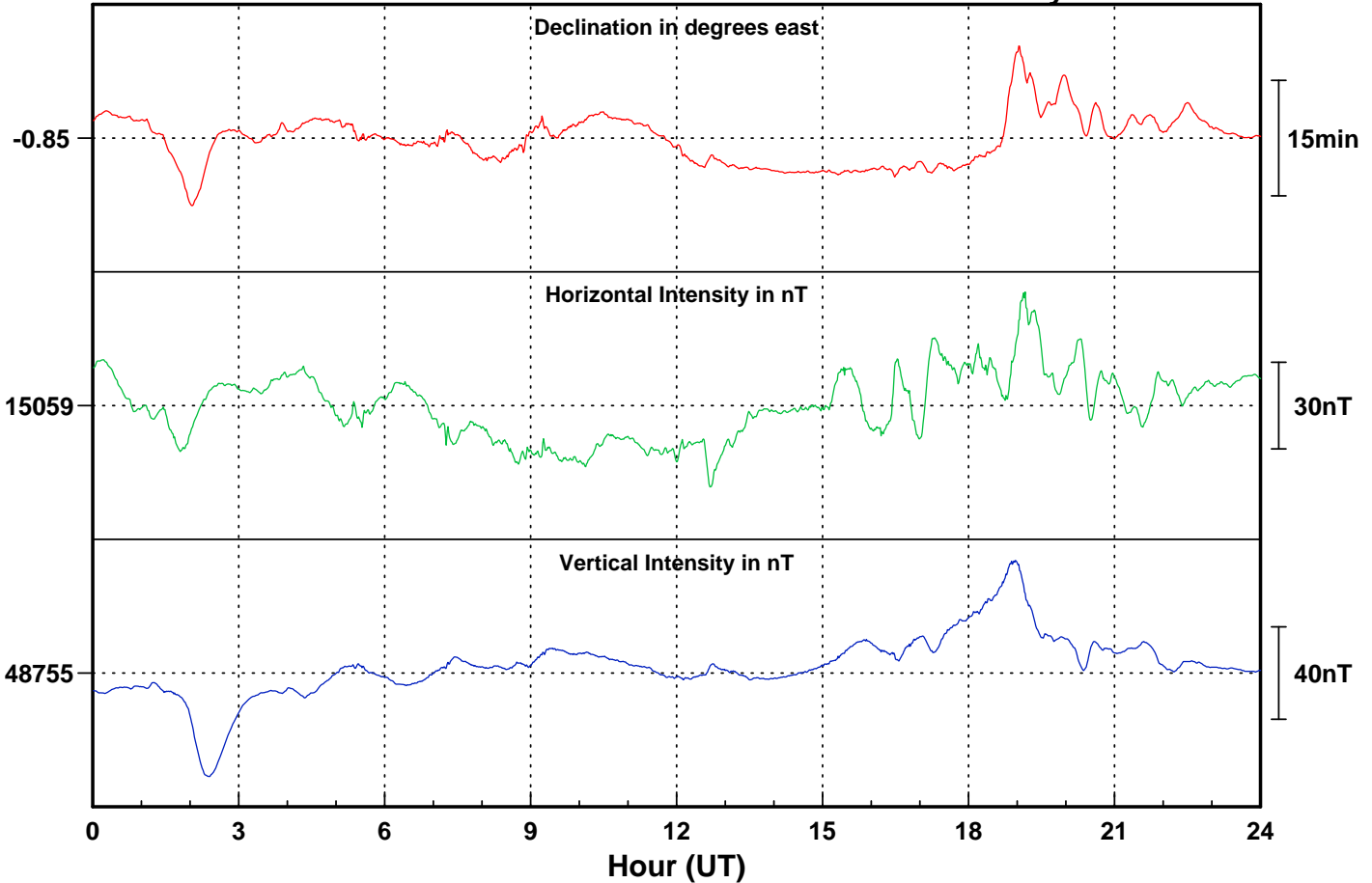
Lerwick

Day number: 246



Date: 04-09-2019

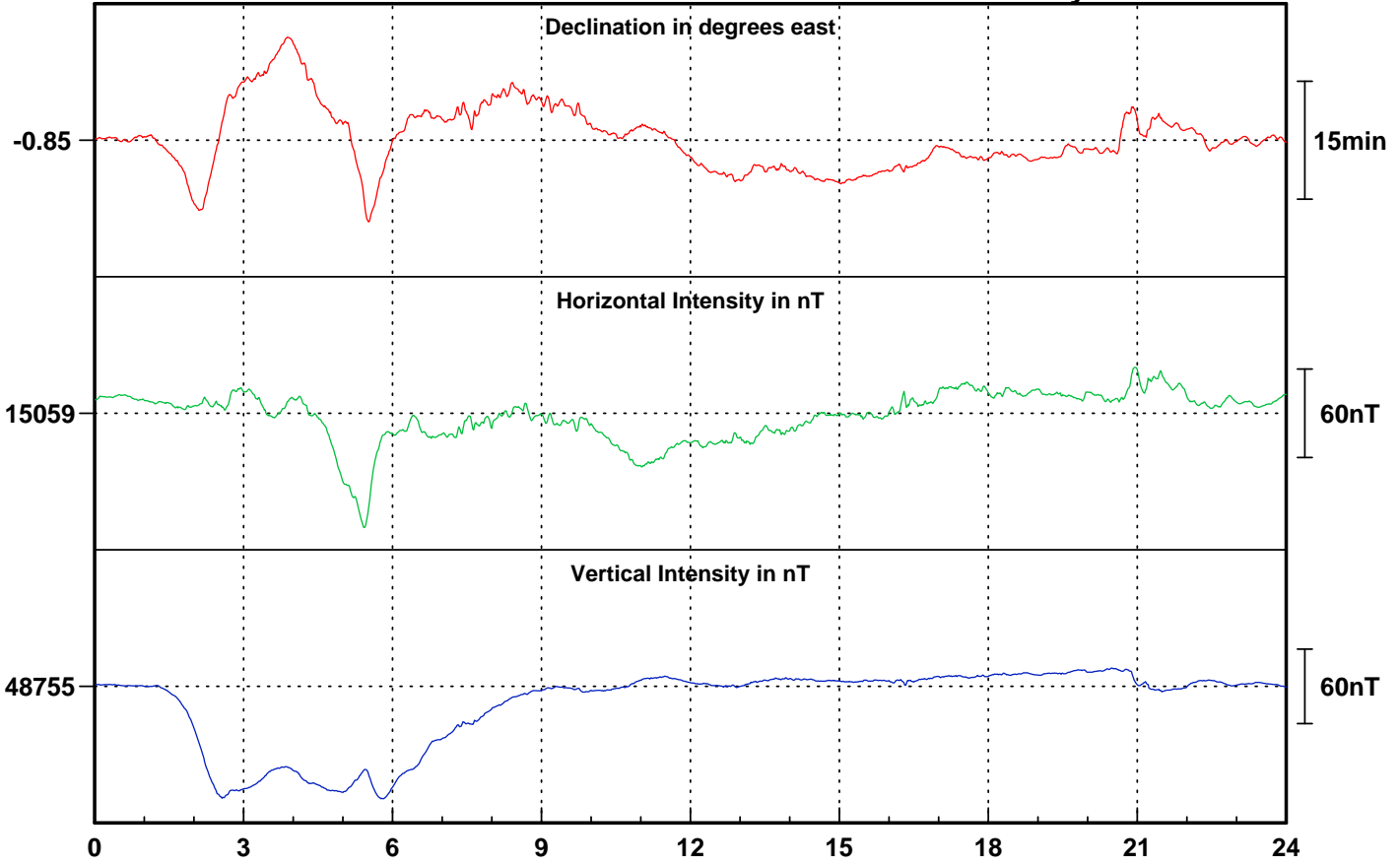
Day number: 247



Date: 05-09-2019

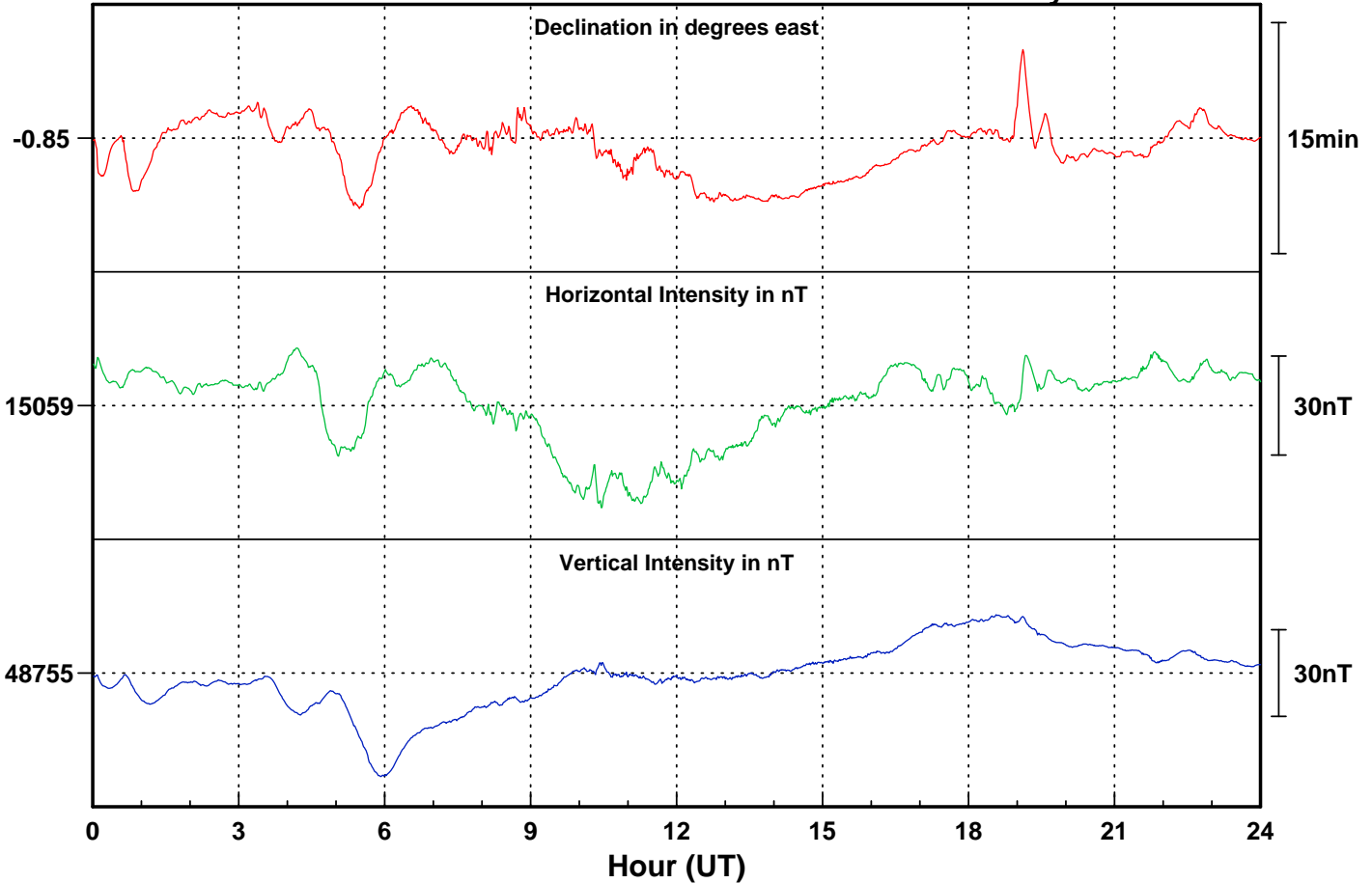
Lerwick

Day number: 248



Date: 06-09-2019

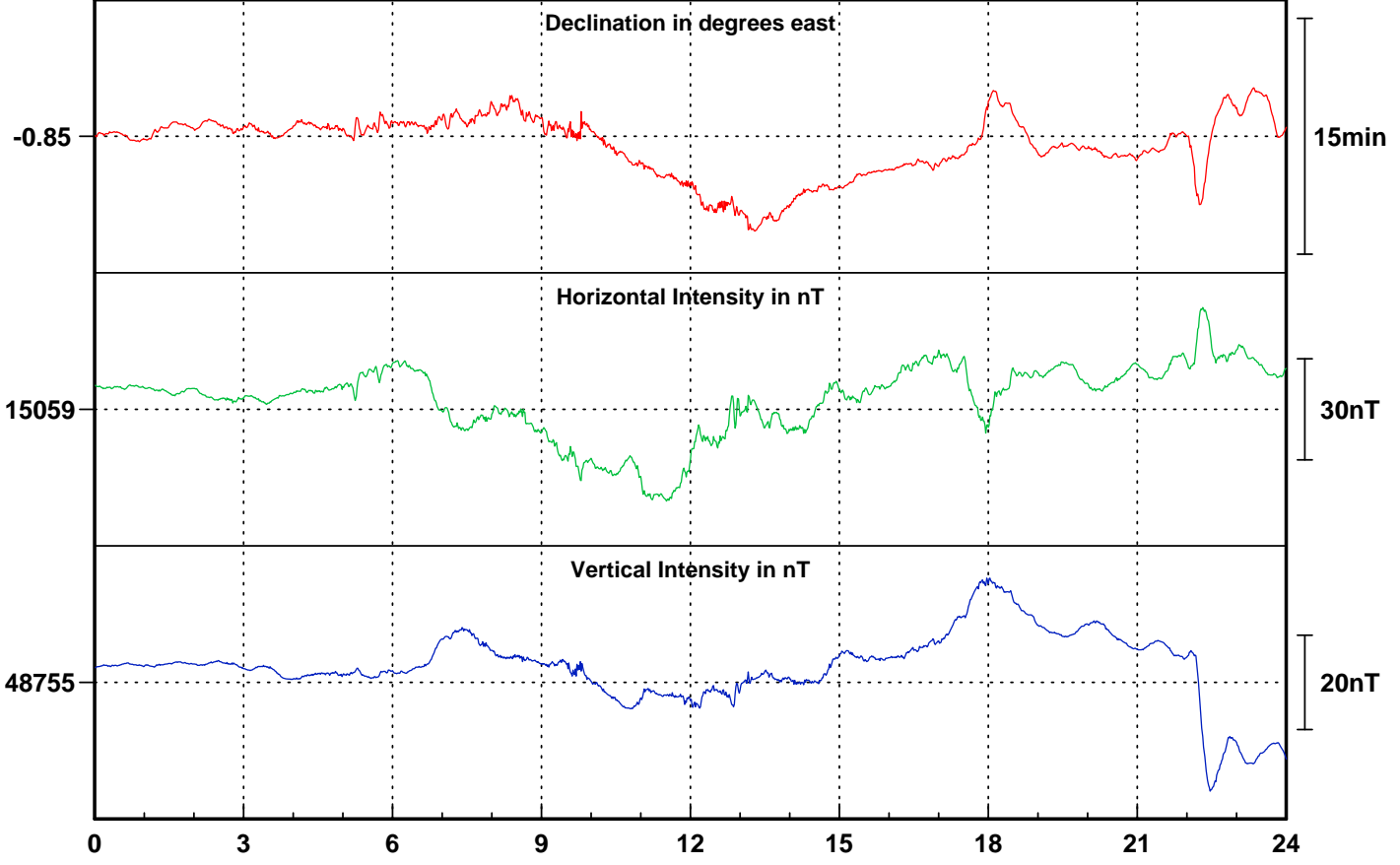
Day number: 249



Date: 07-09-2019

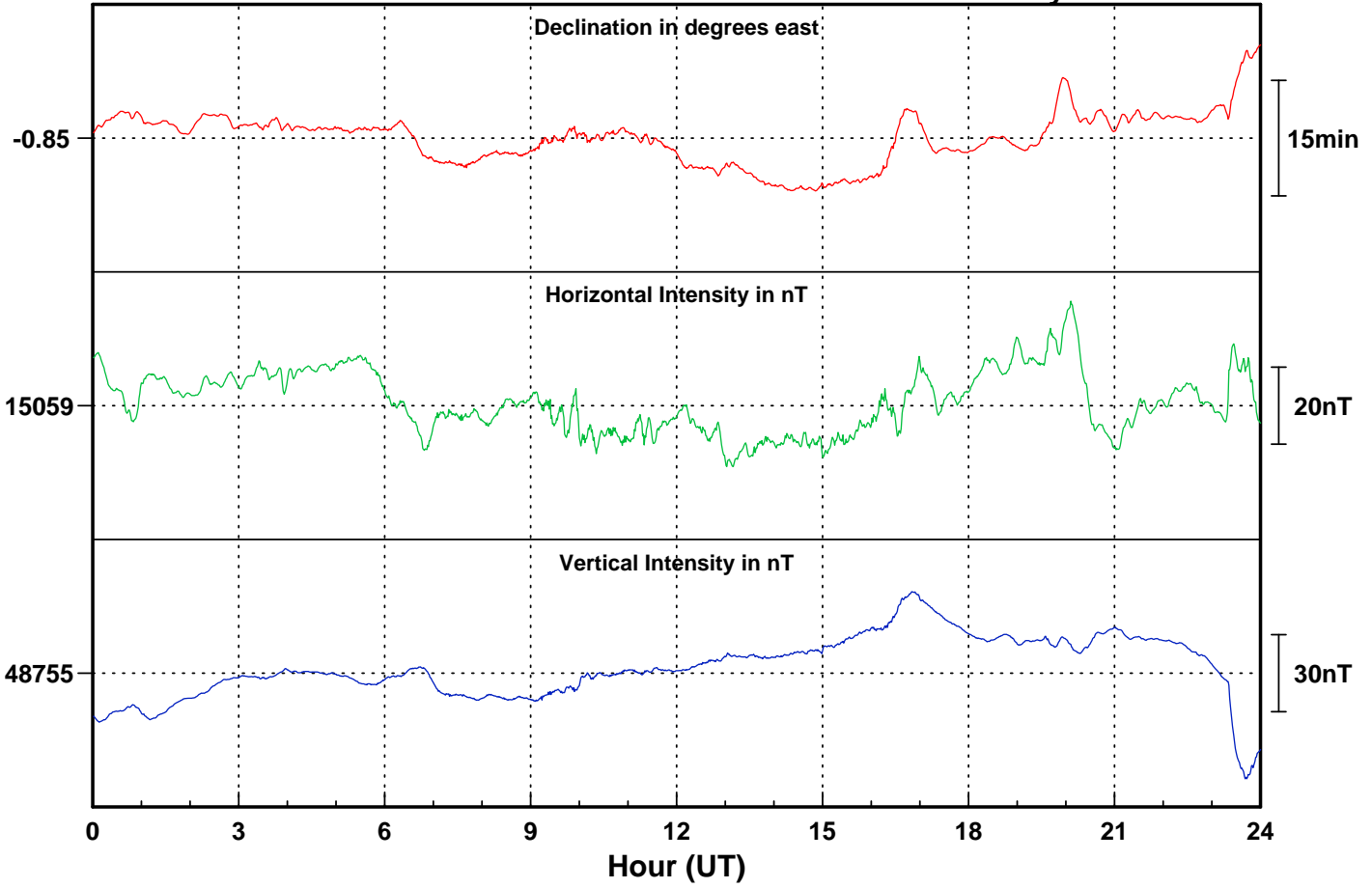
Lerwick

Day number: 250



Date: 08-09-2019

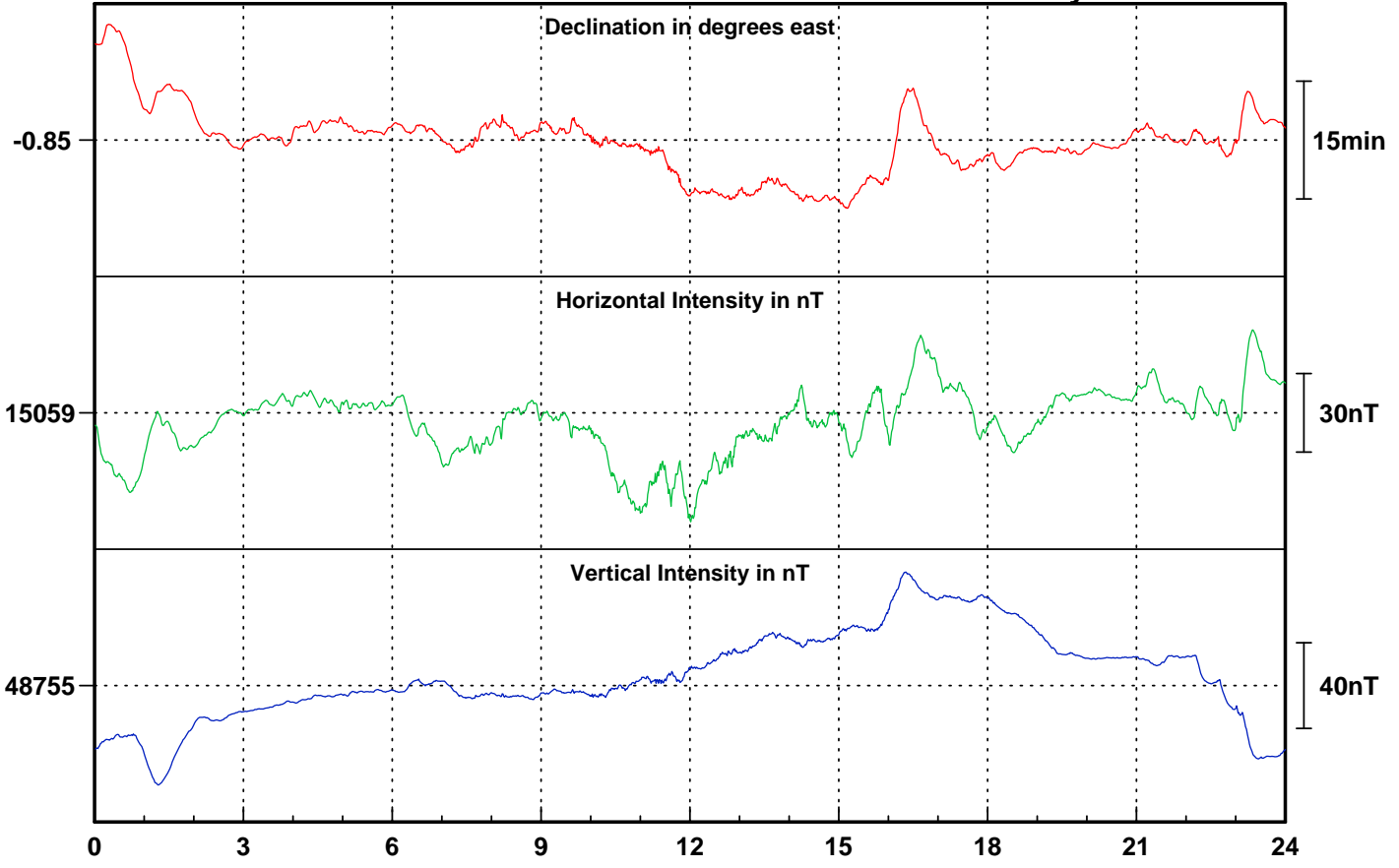
Day number: 251



Date: 09-09-2019

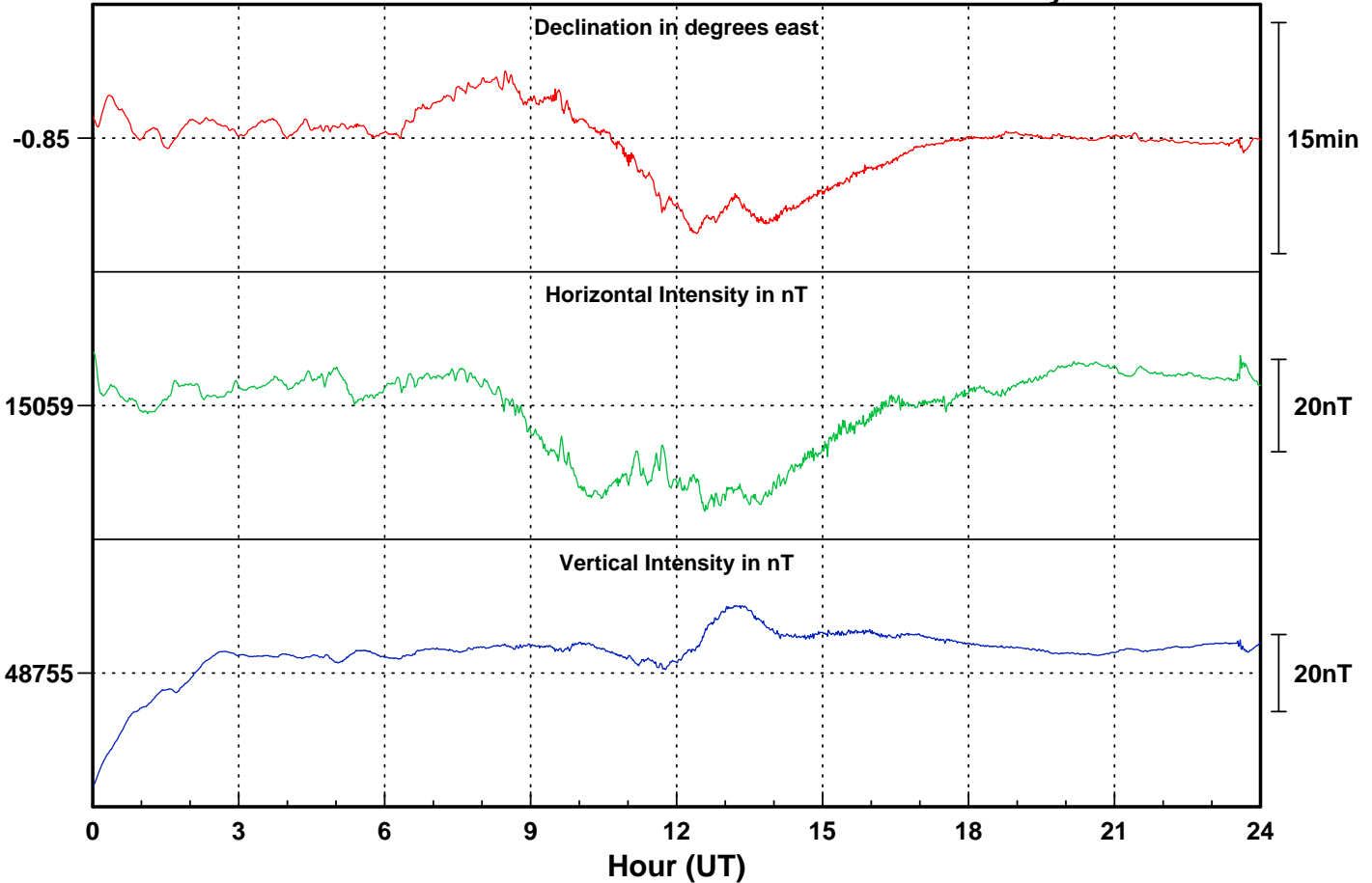
Lerwick

Day number: 252



Date: 10-09-2019

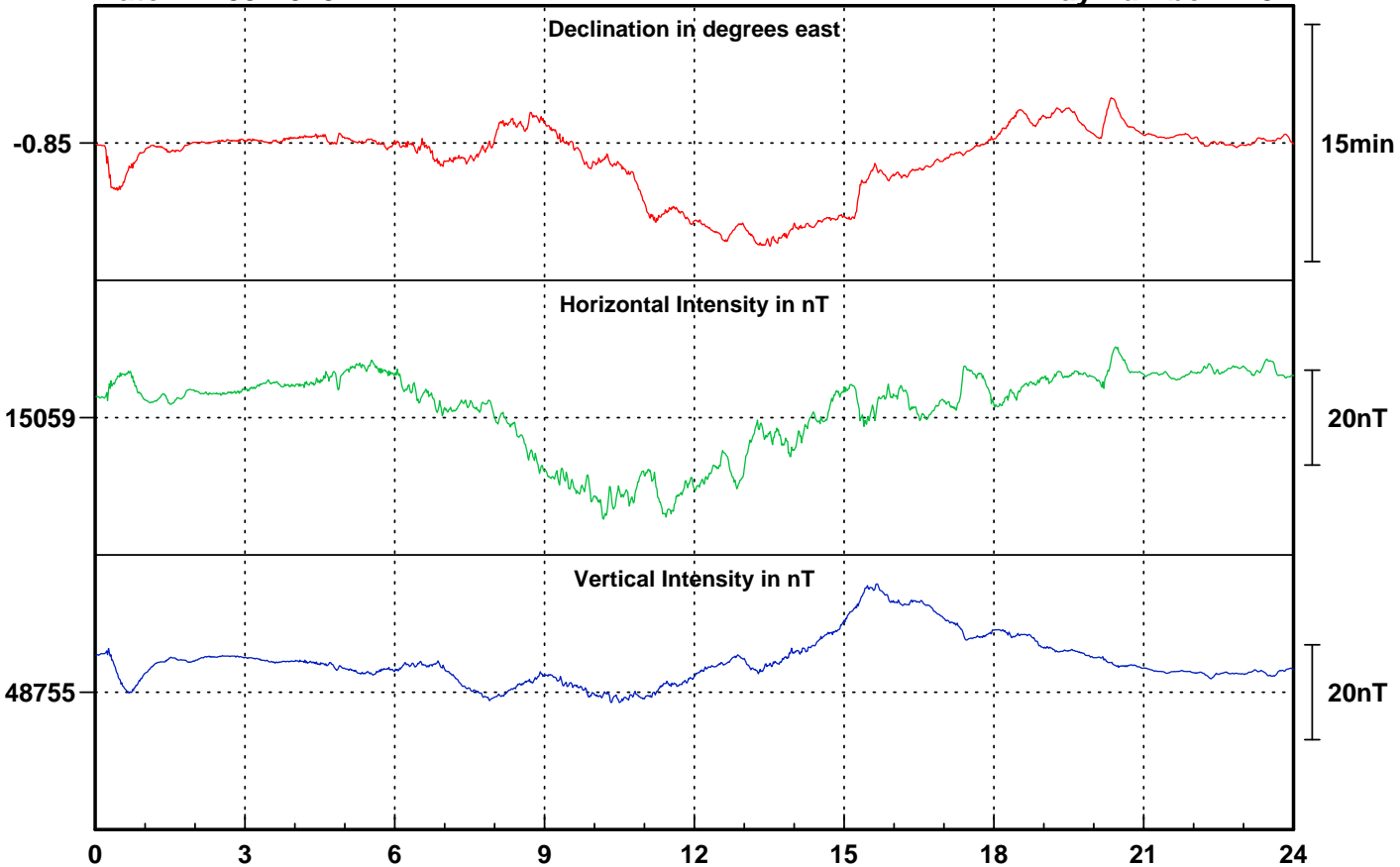
Day number: 253



Date: 11-09-2019

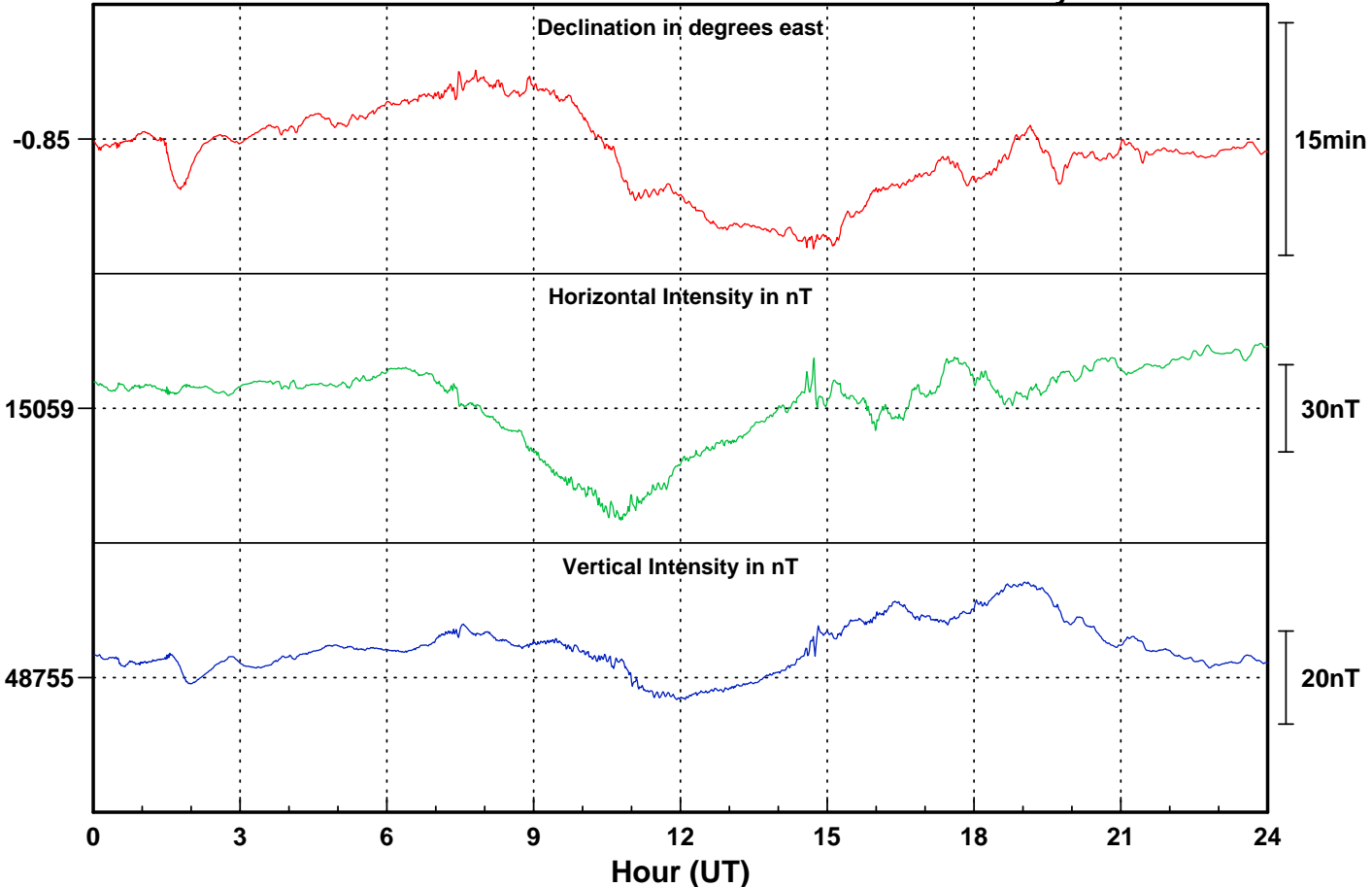
Lerwick

Day number: 254



Date: 12-09-2019

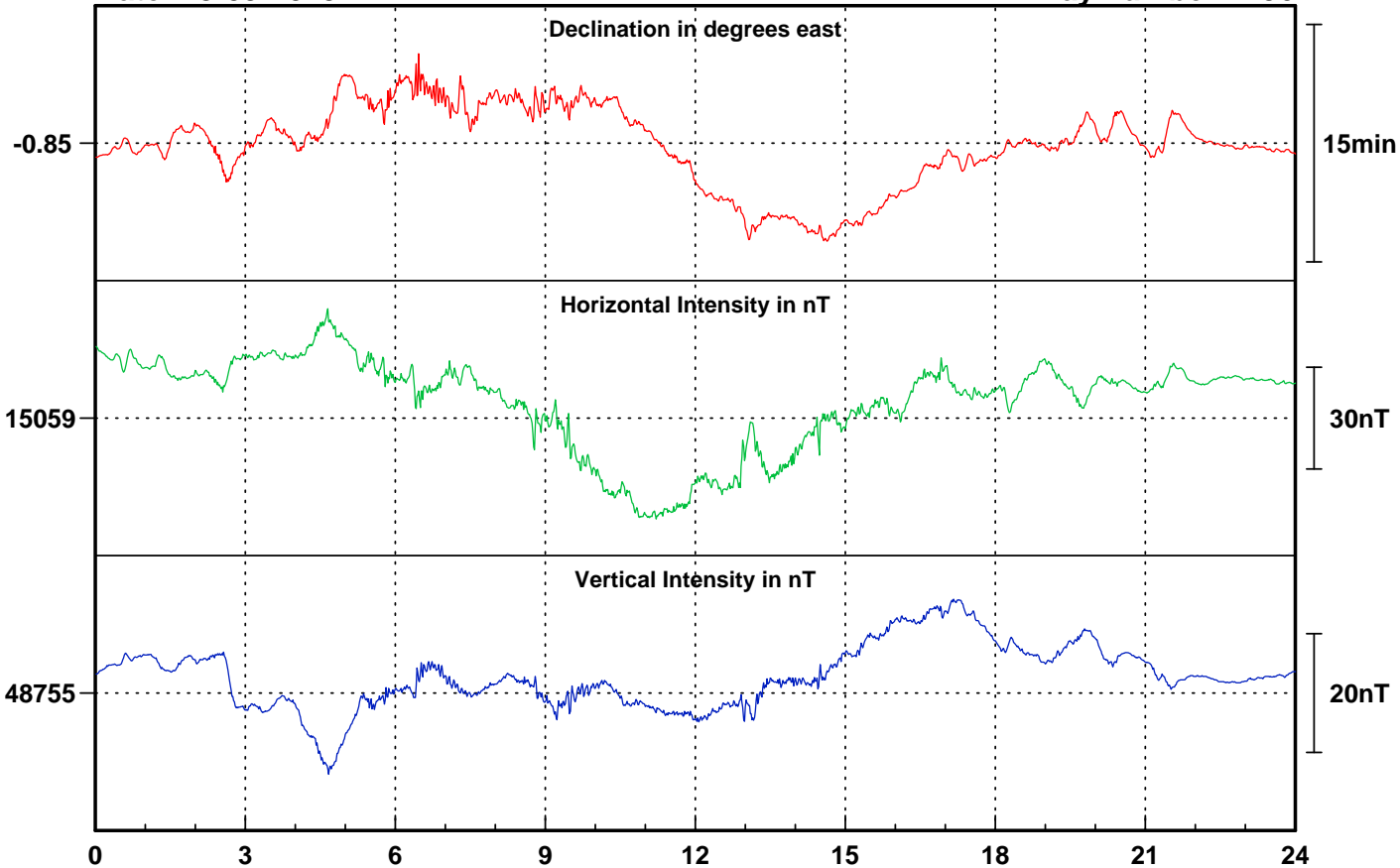
Day number: 255



Date: 13-09-2019

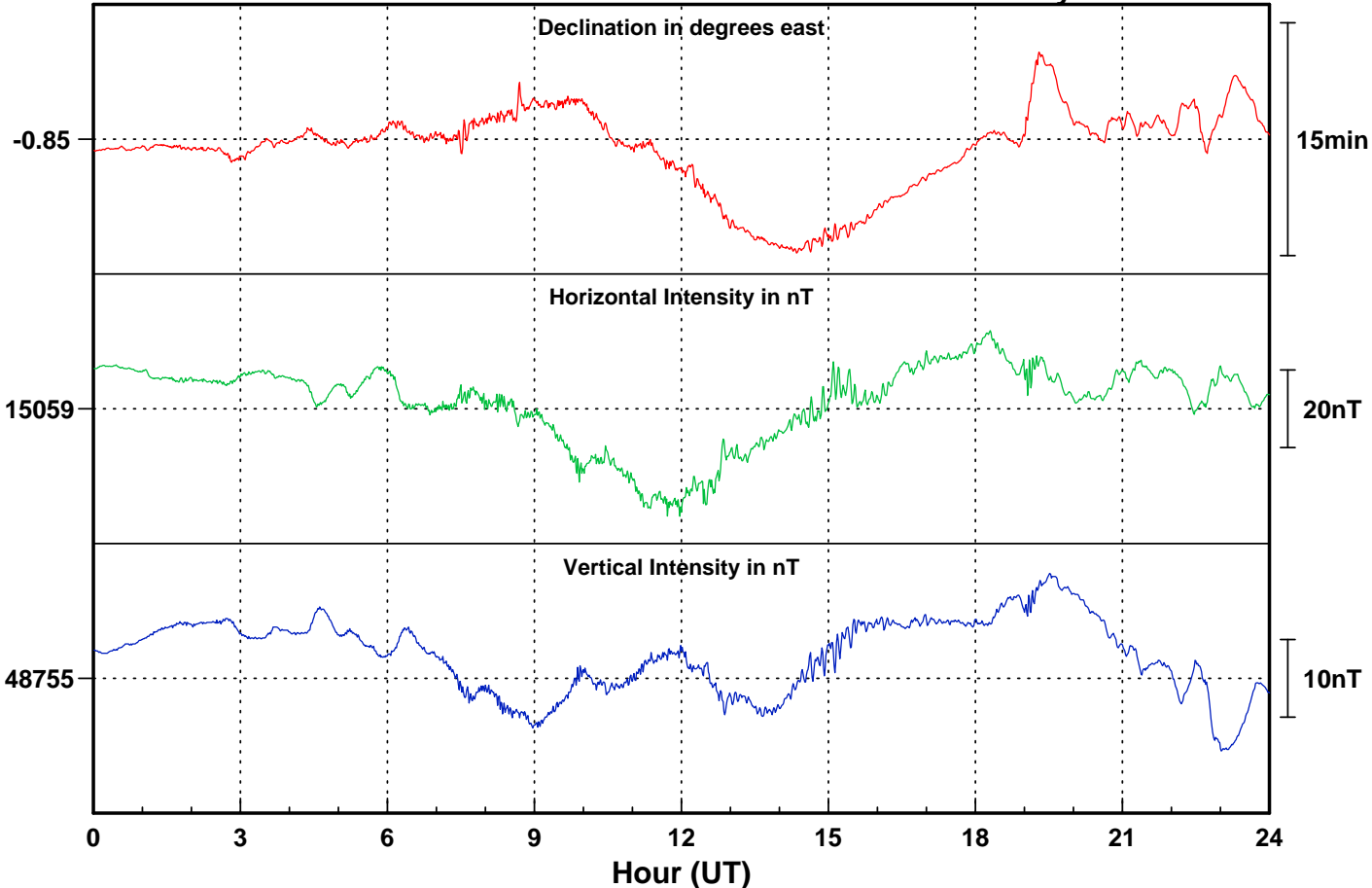
Lerwick

Day number: 256



Date: 14-09-2019

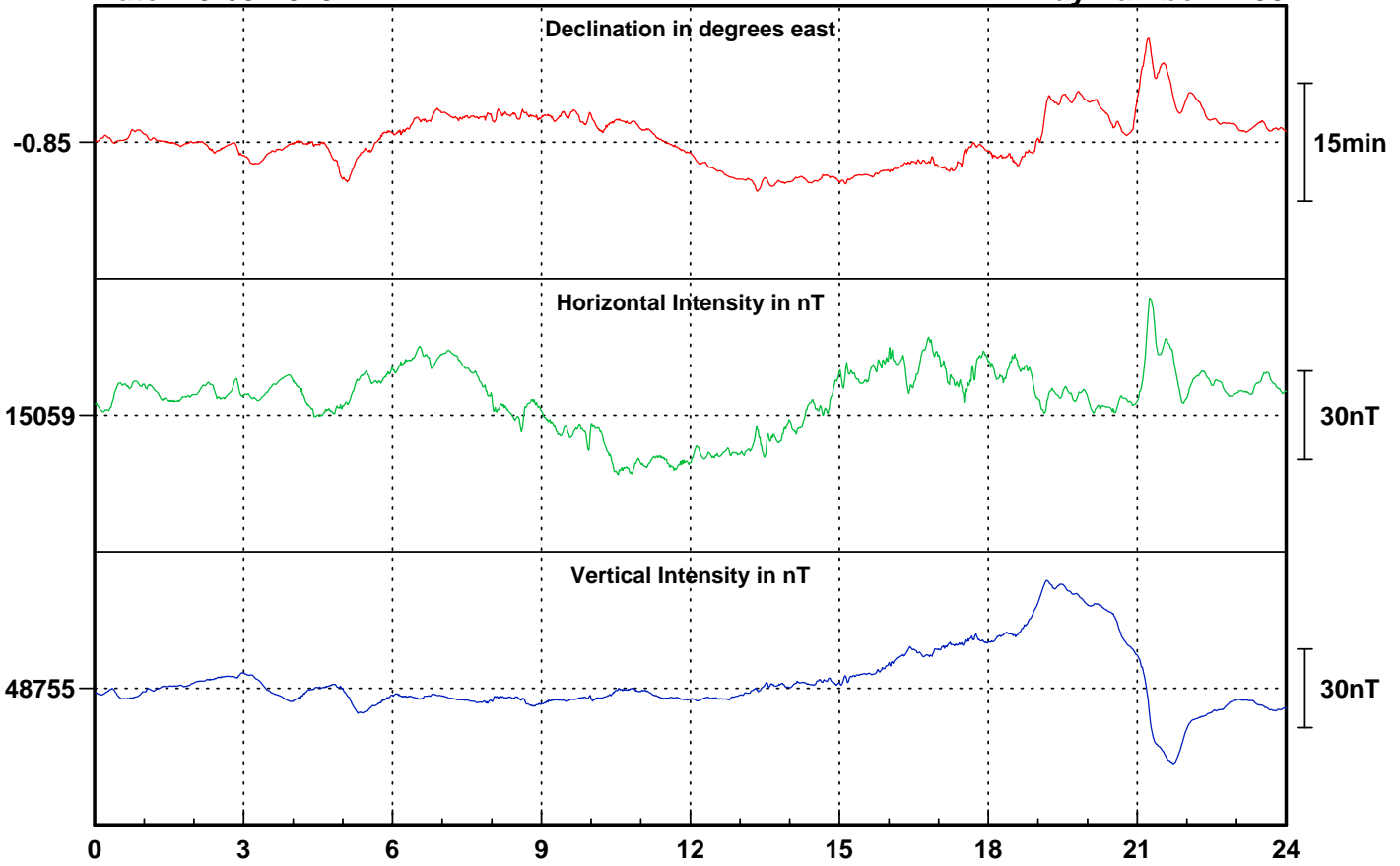
Day number: 257



Date: 15-09-2019

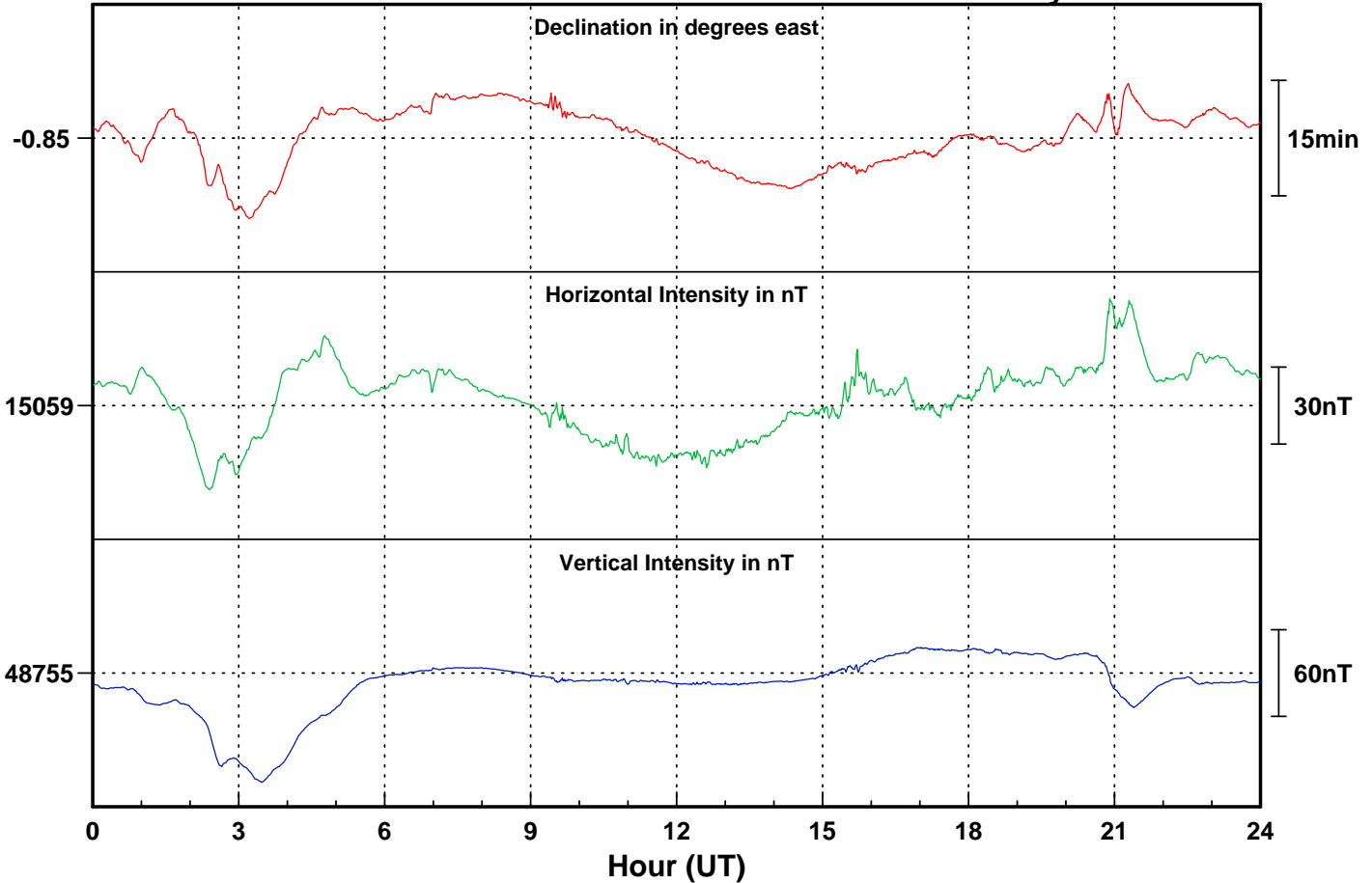
Lerwick

Day number: 258



Date: 16-09-2019

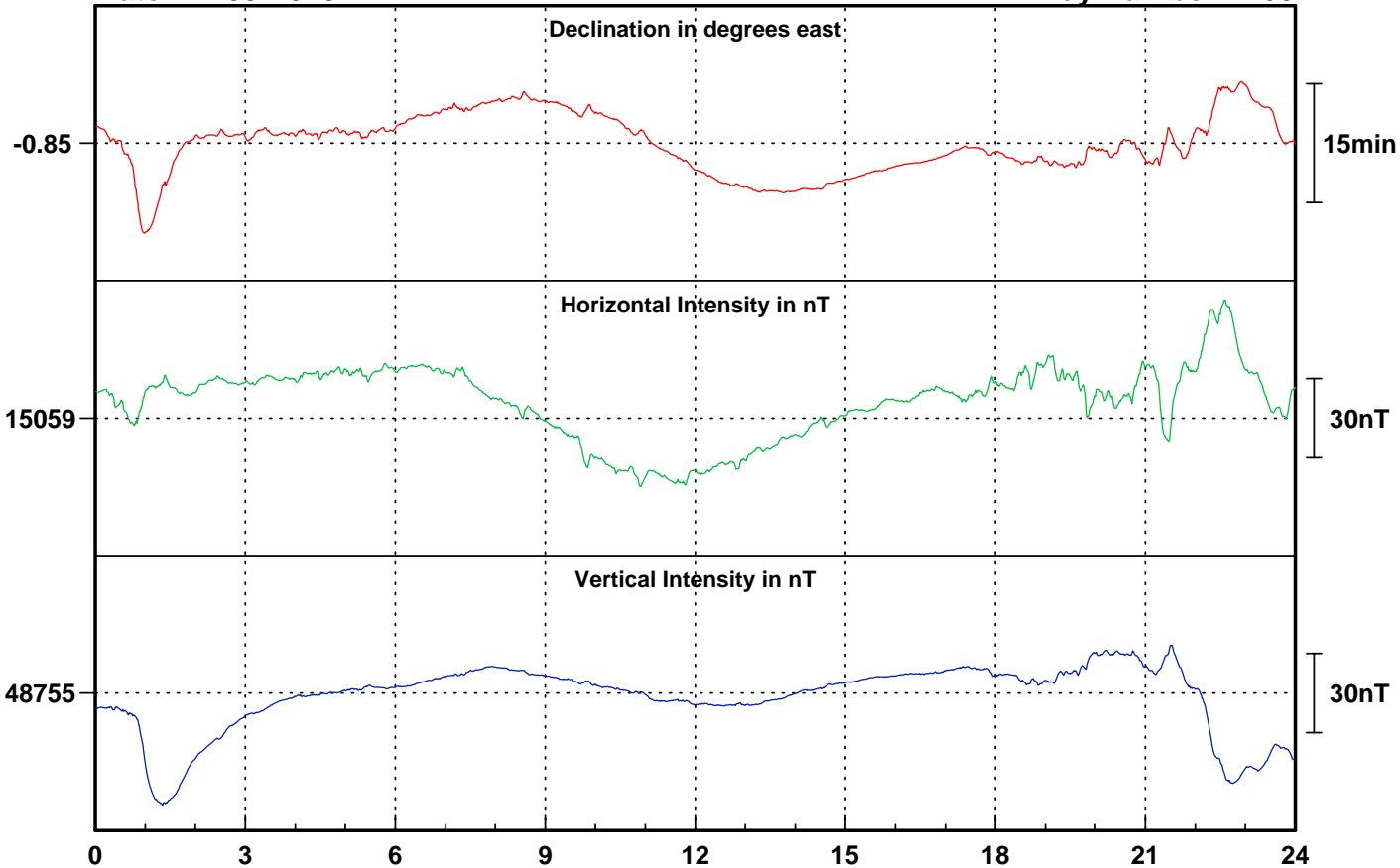
Day number: 259



Date: 17-09-2019

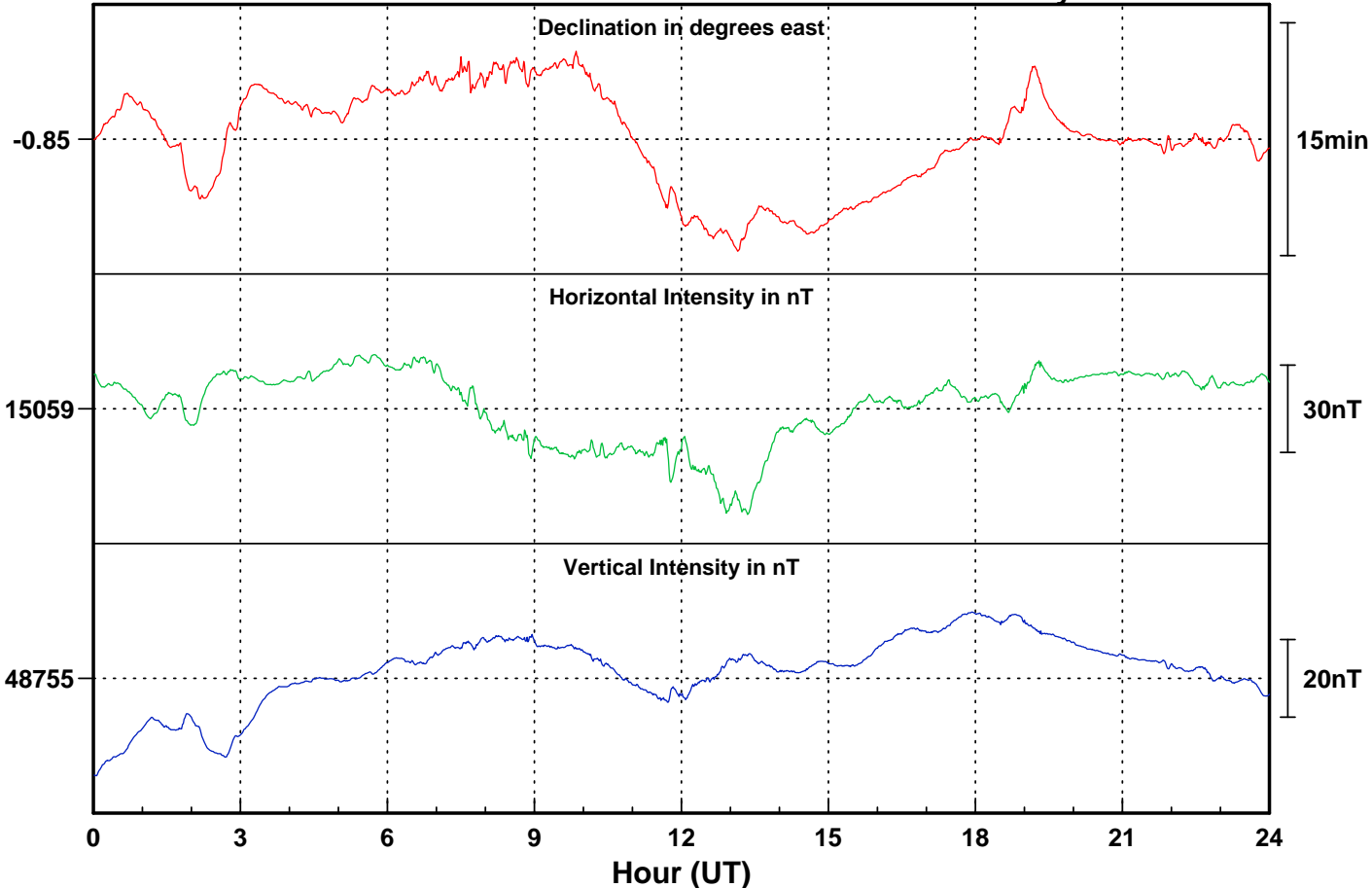
Lerwick

Day number: 260



Date: 18-09-2019

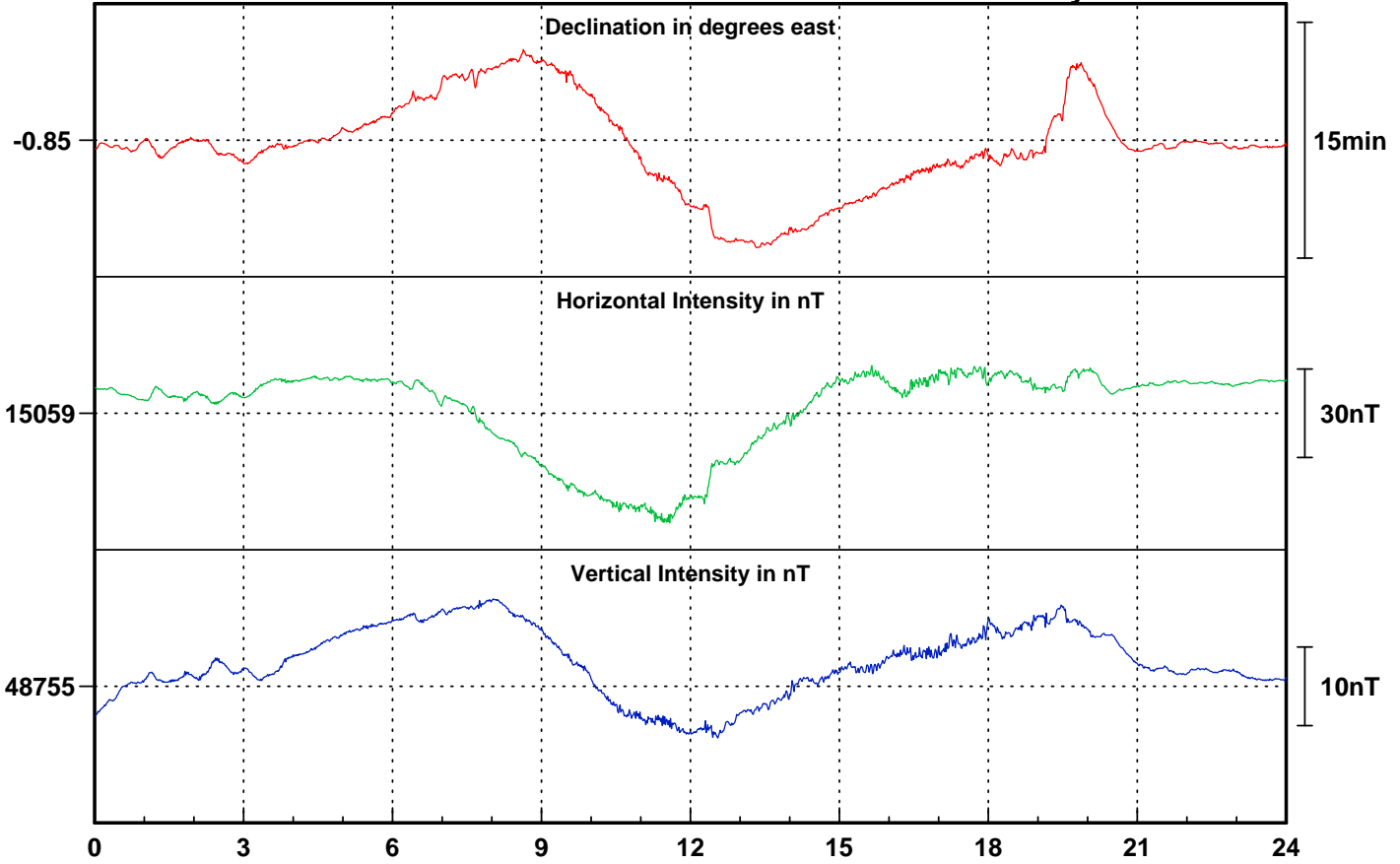
Day number: 261



Date: 19-09-2019

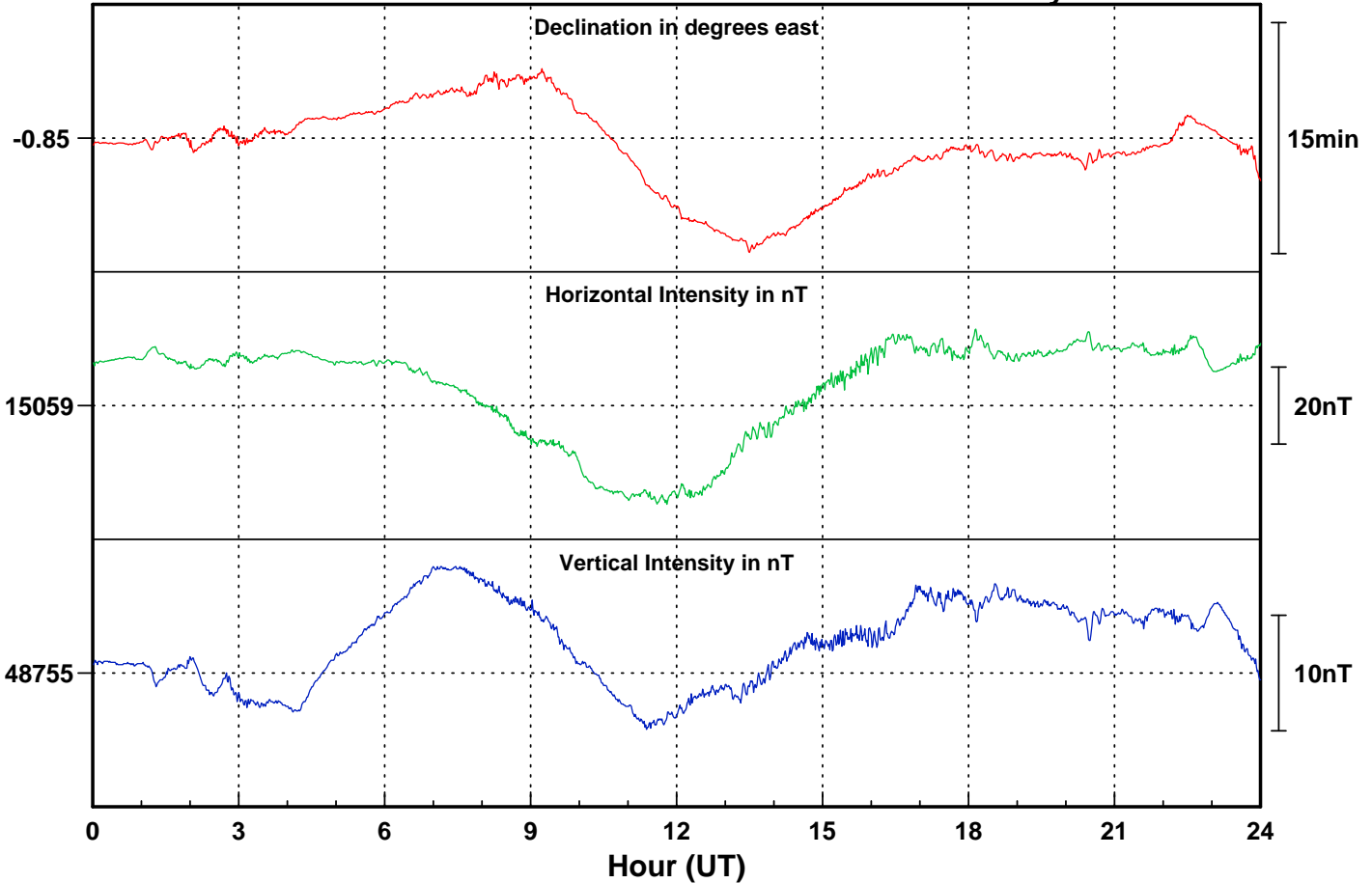
Lerwick

Day number: 262



Date: 20-09-2019

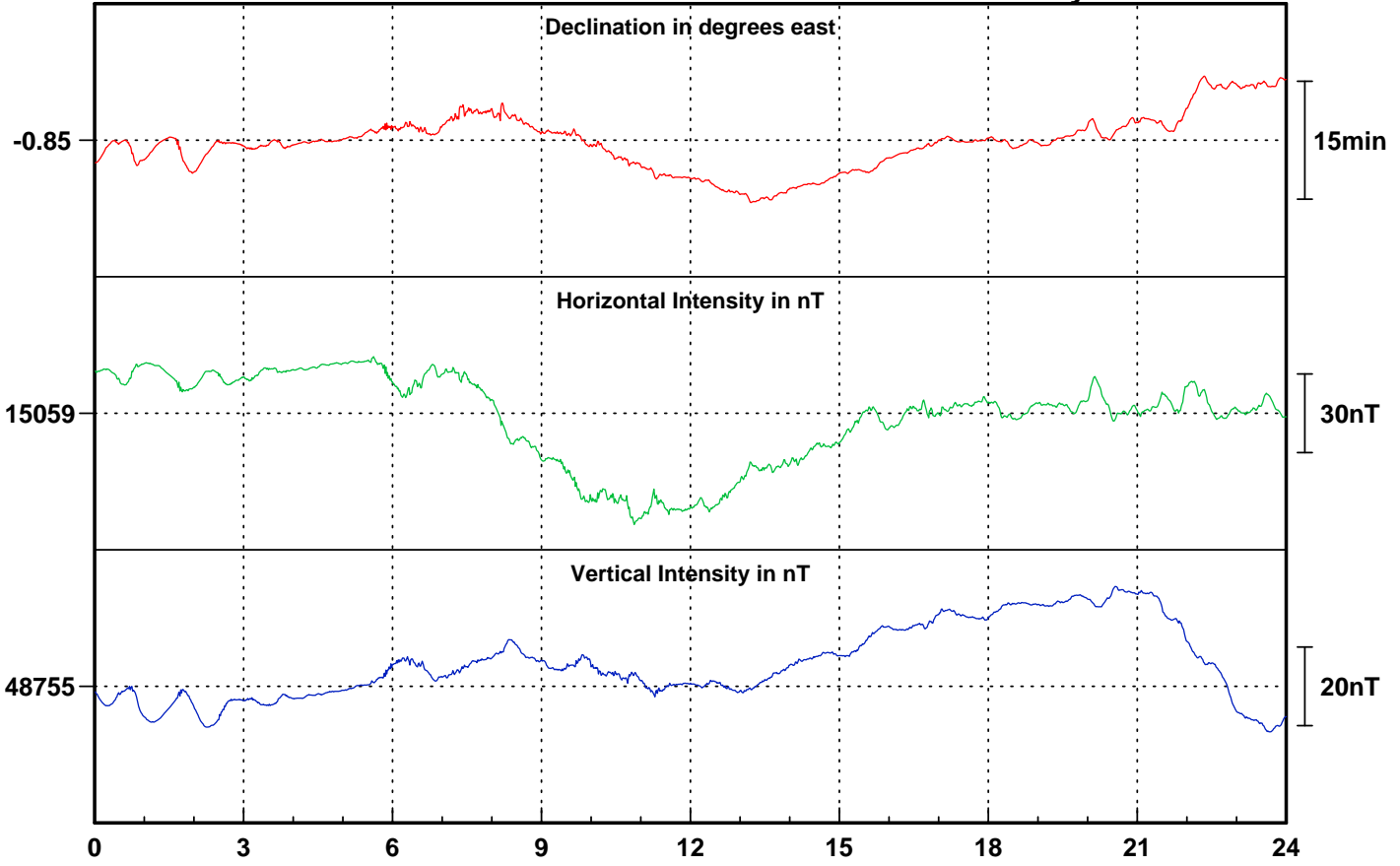
Day number: 263



Date: 21-09-2019

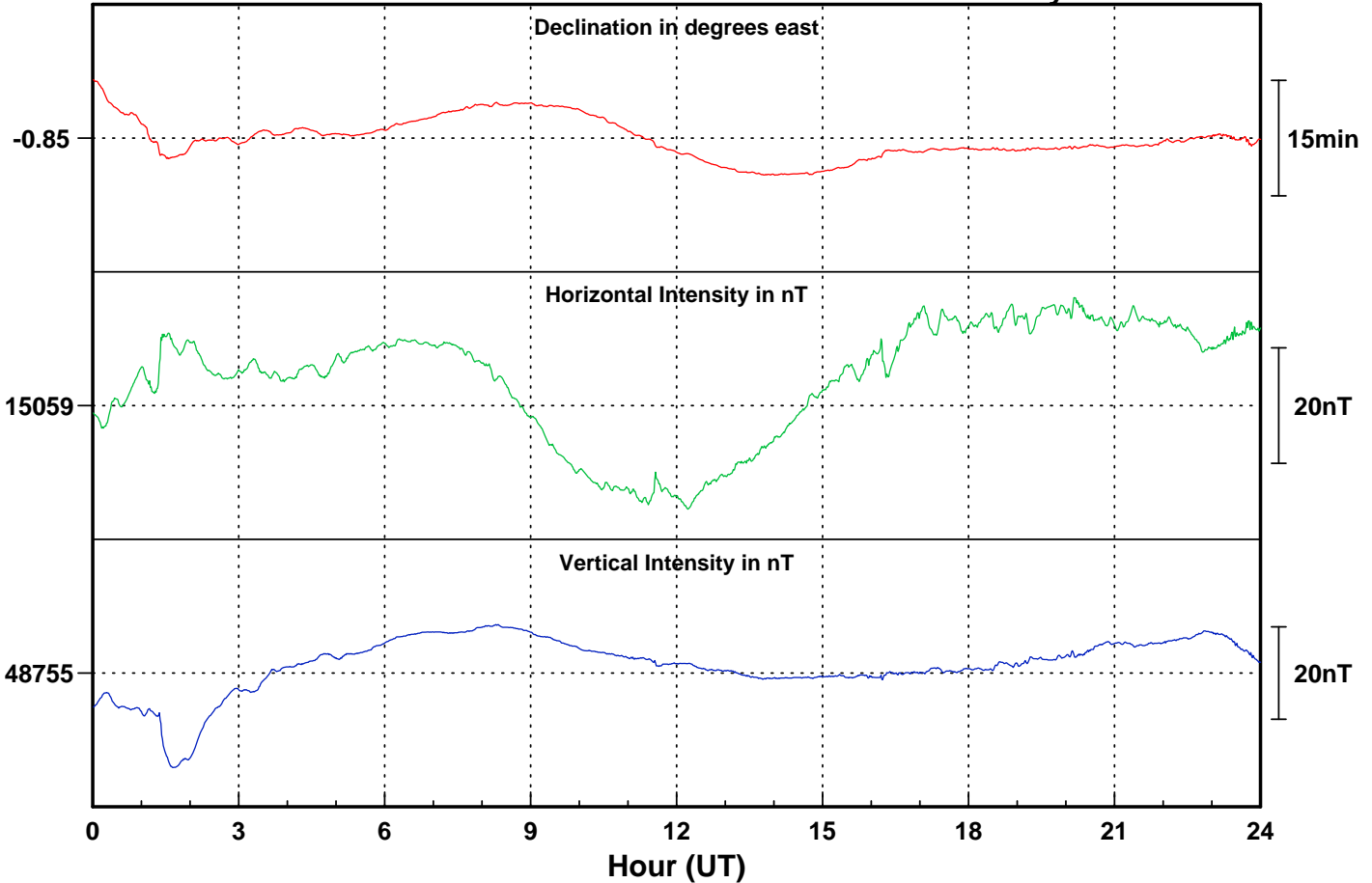
Lerwick

Day number: 264



Date: 22-09-2019

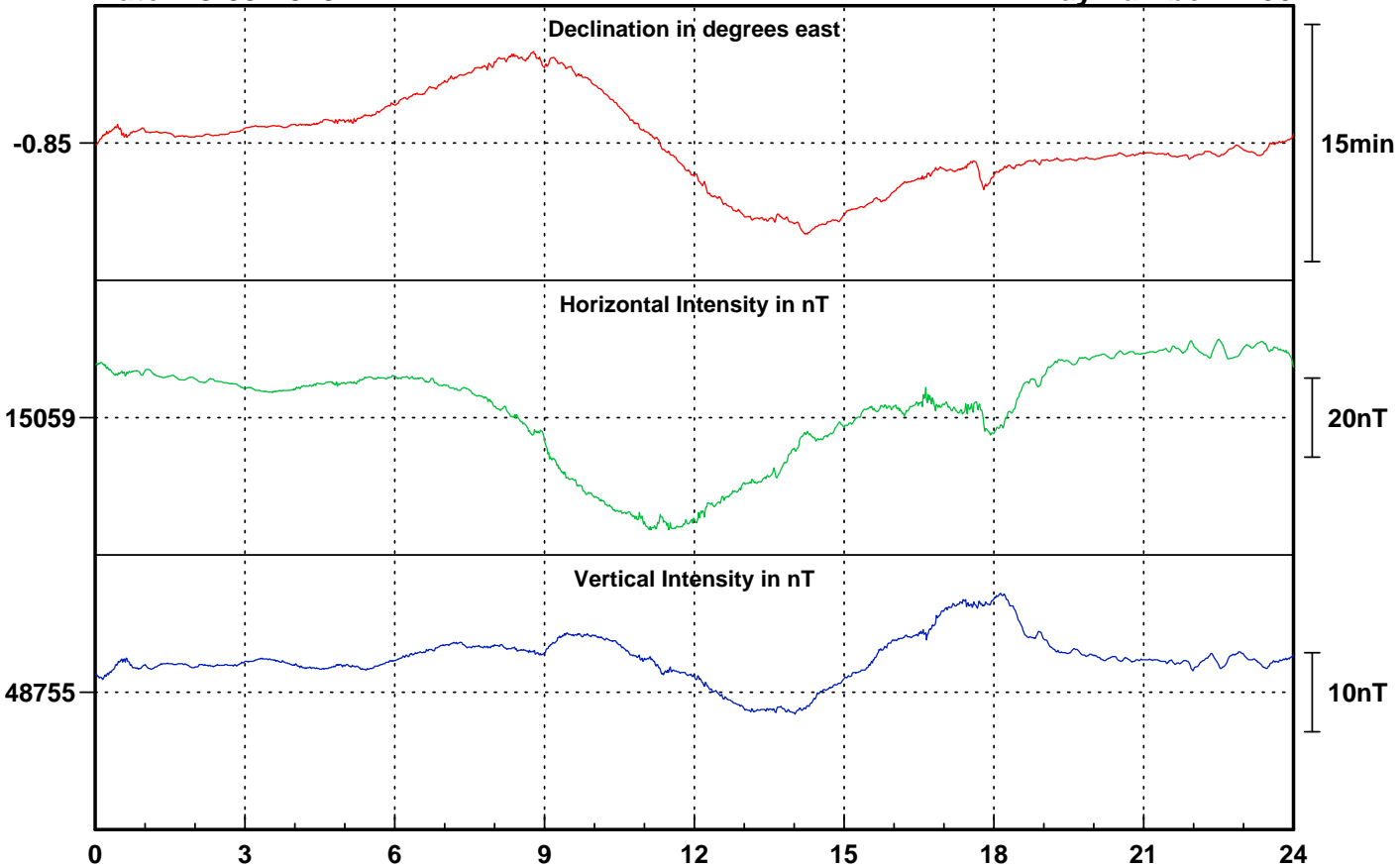
Day number: 265



Date: 23-09-2019

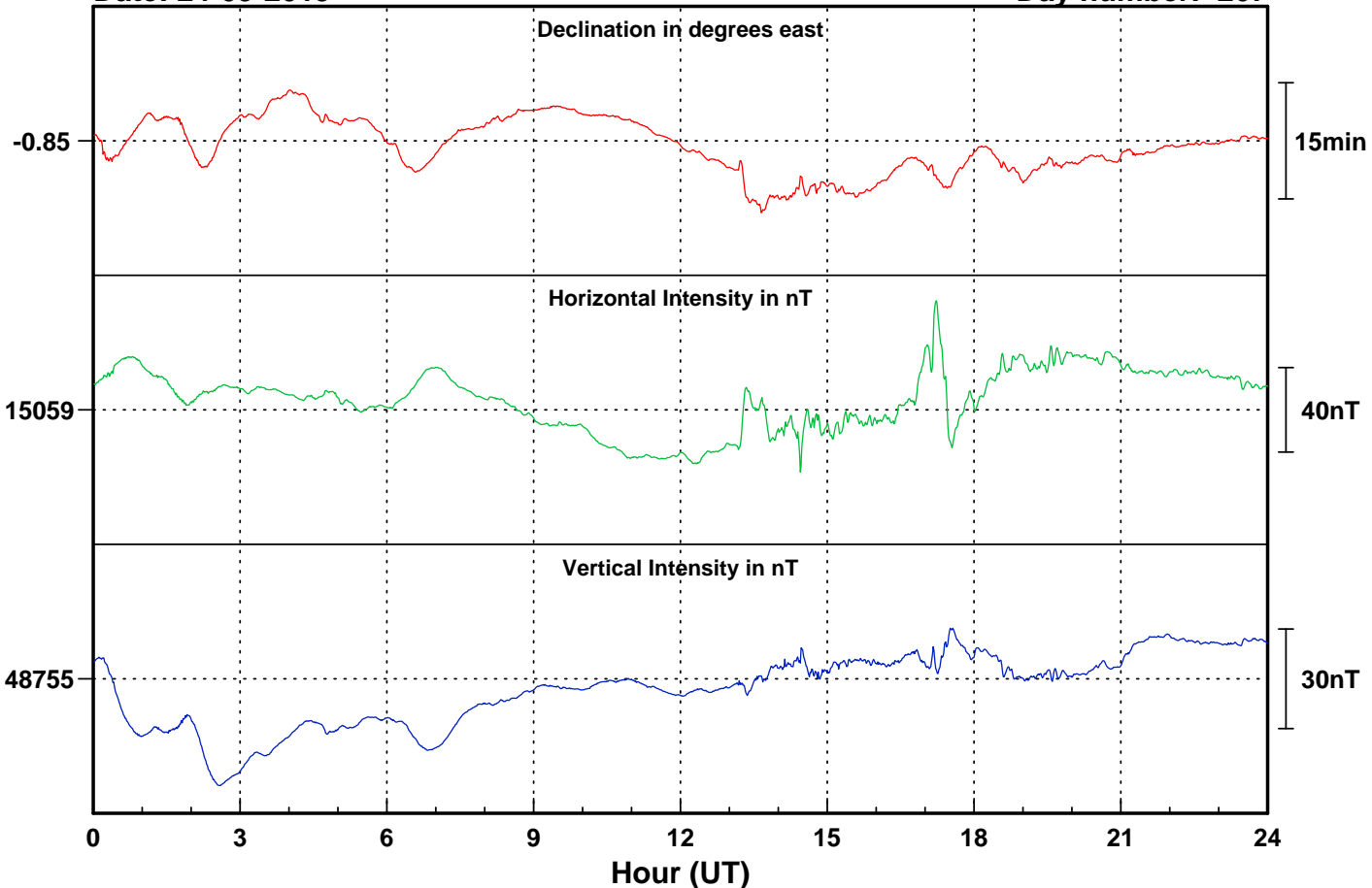
Lerwick

Day number: 266



Date: 24-09-2019

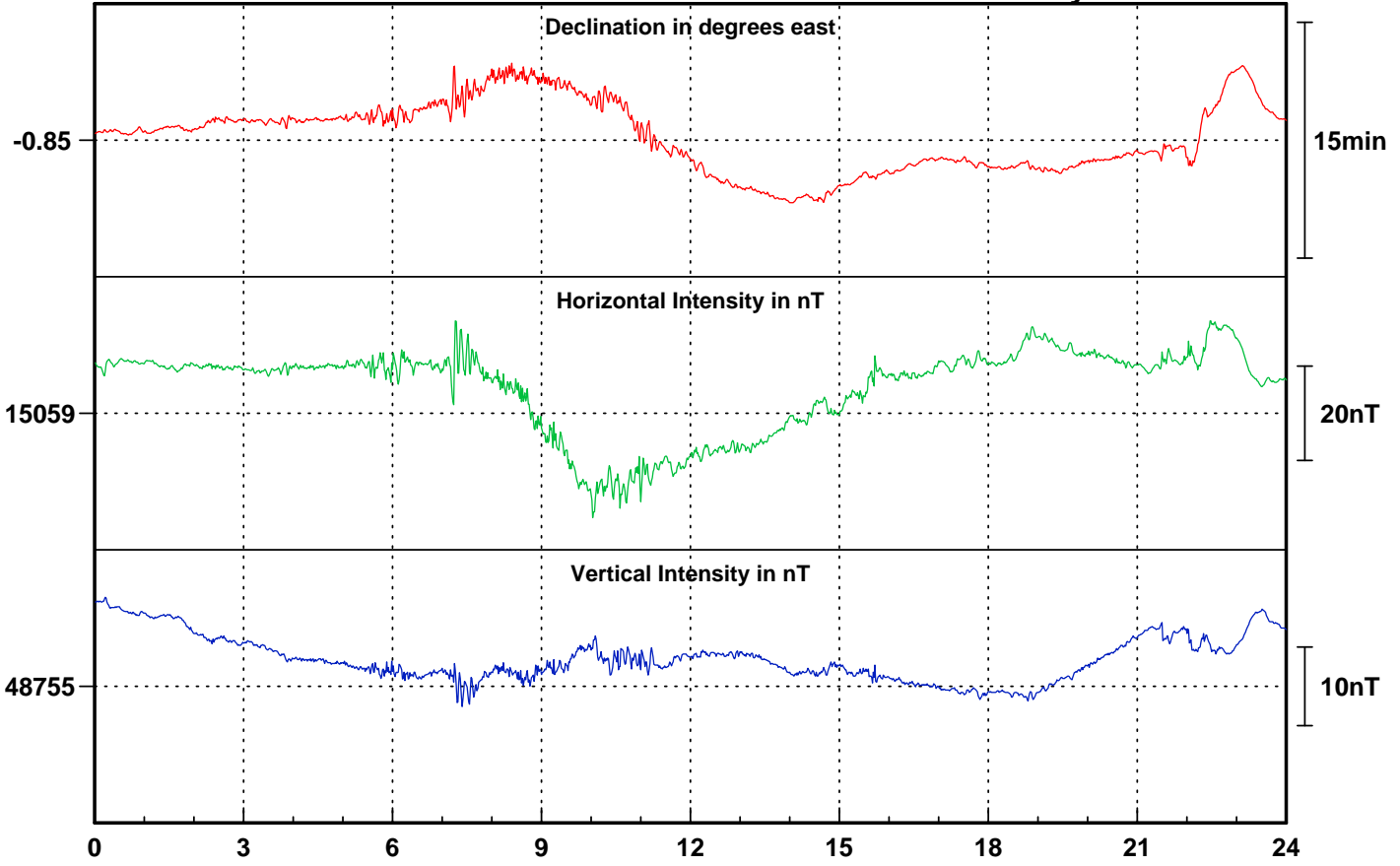
Day number: 267



Date: 25-09-2019

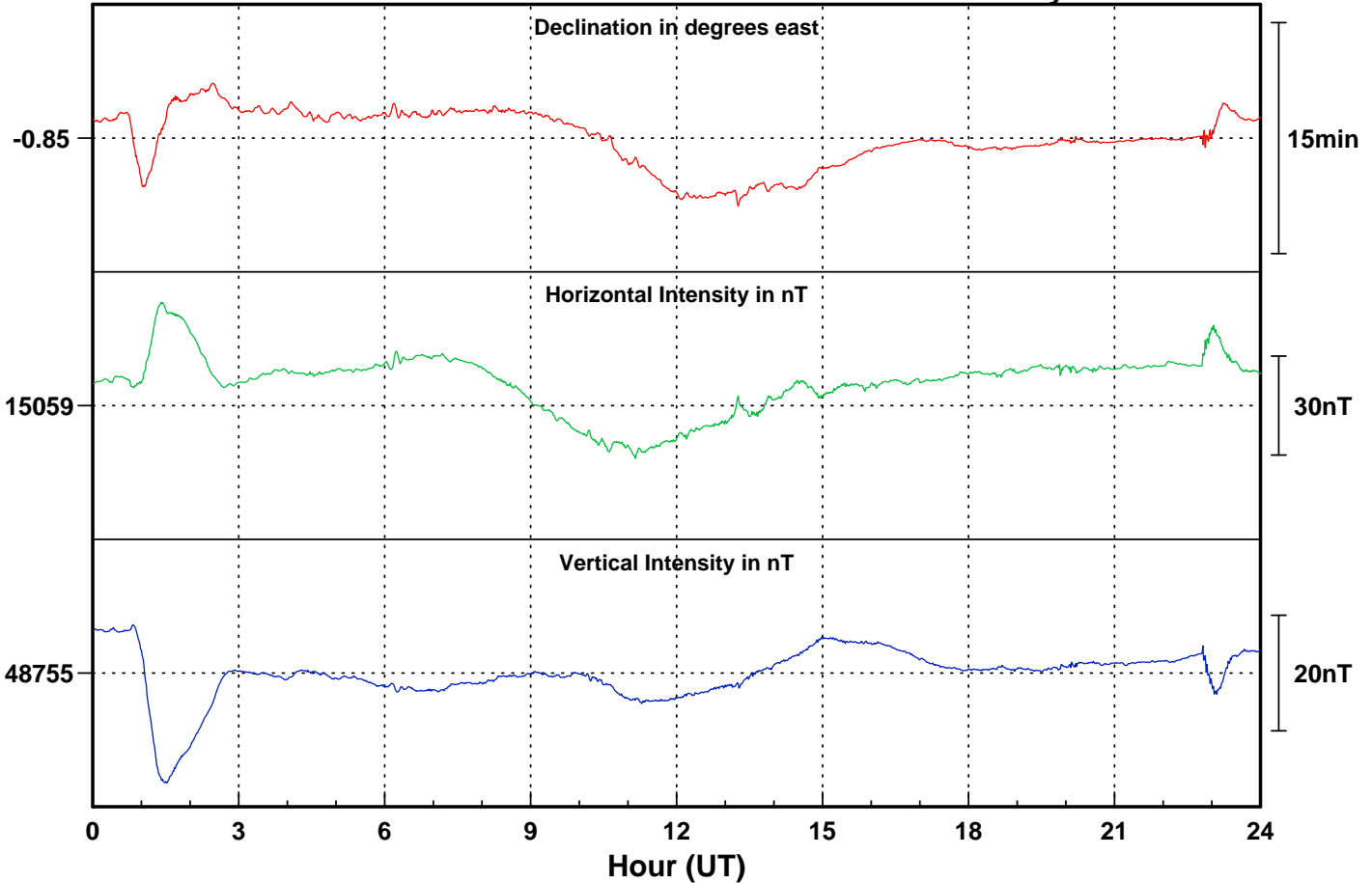
Lerwick

Day number: 268



Date: 26-09-2019

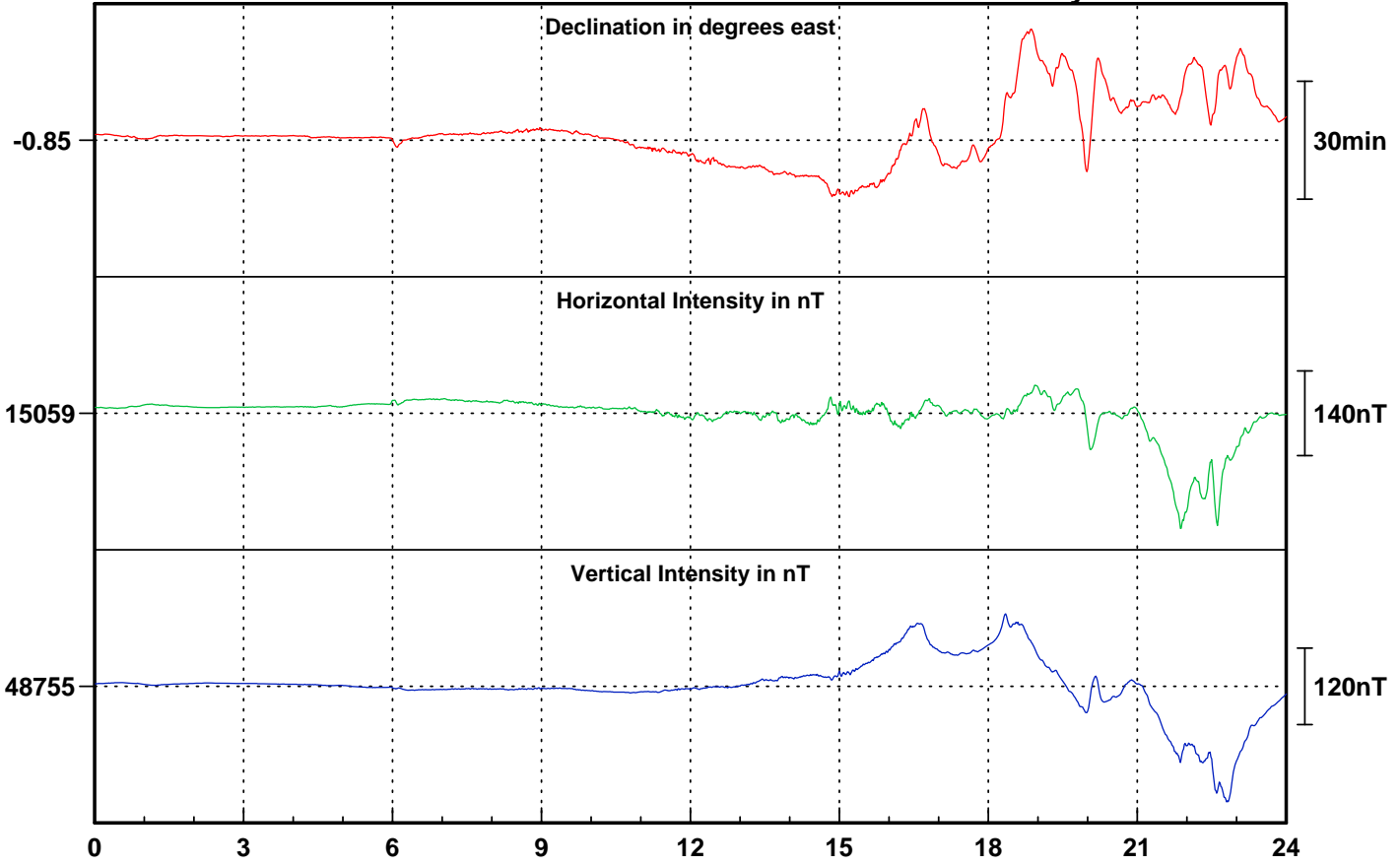
Day number: 269



Date: 27-09-2019

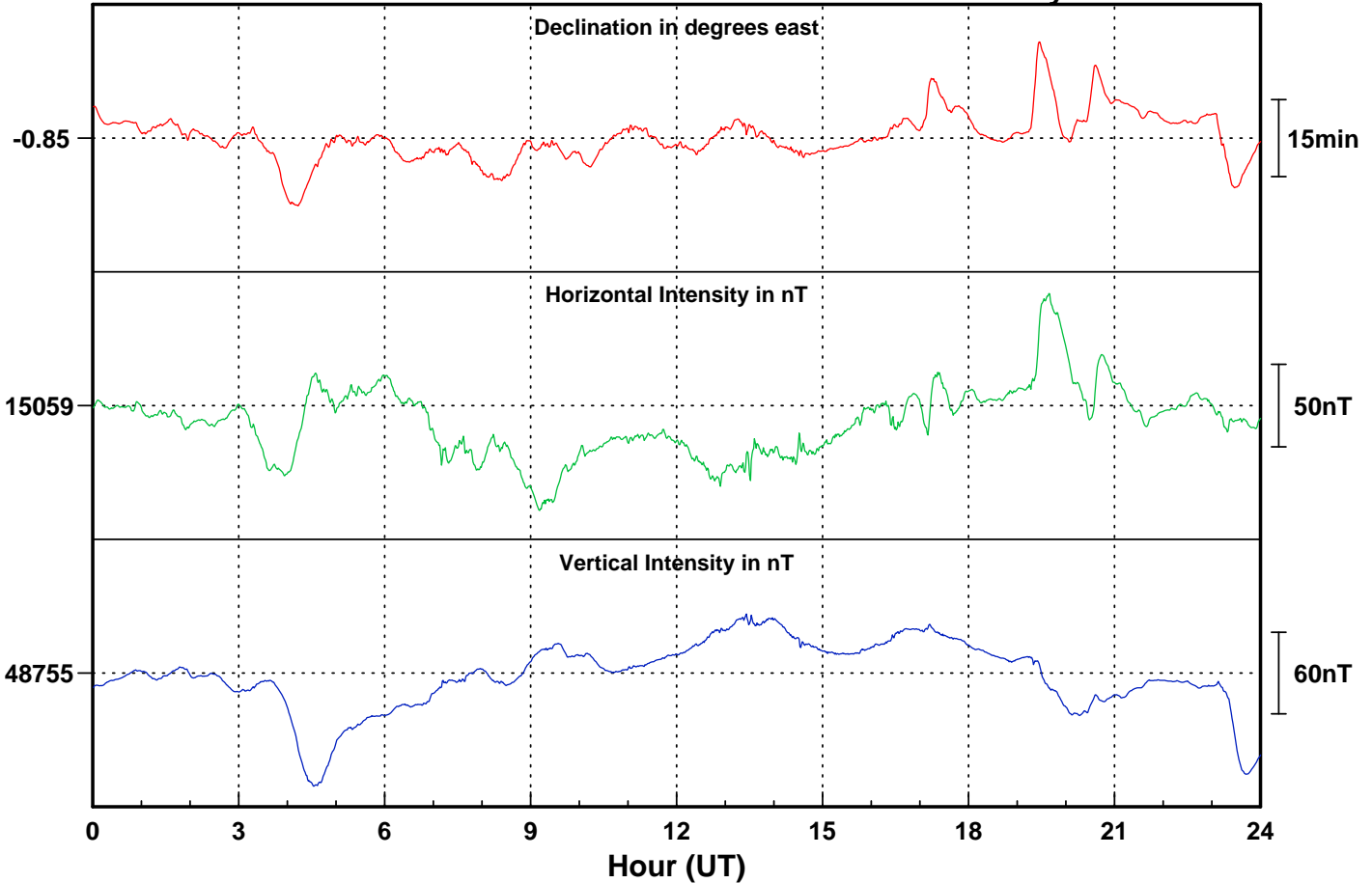
Lerwick

Day number: 270



Date: 28-09-2019

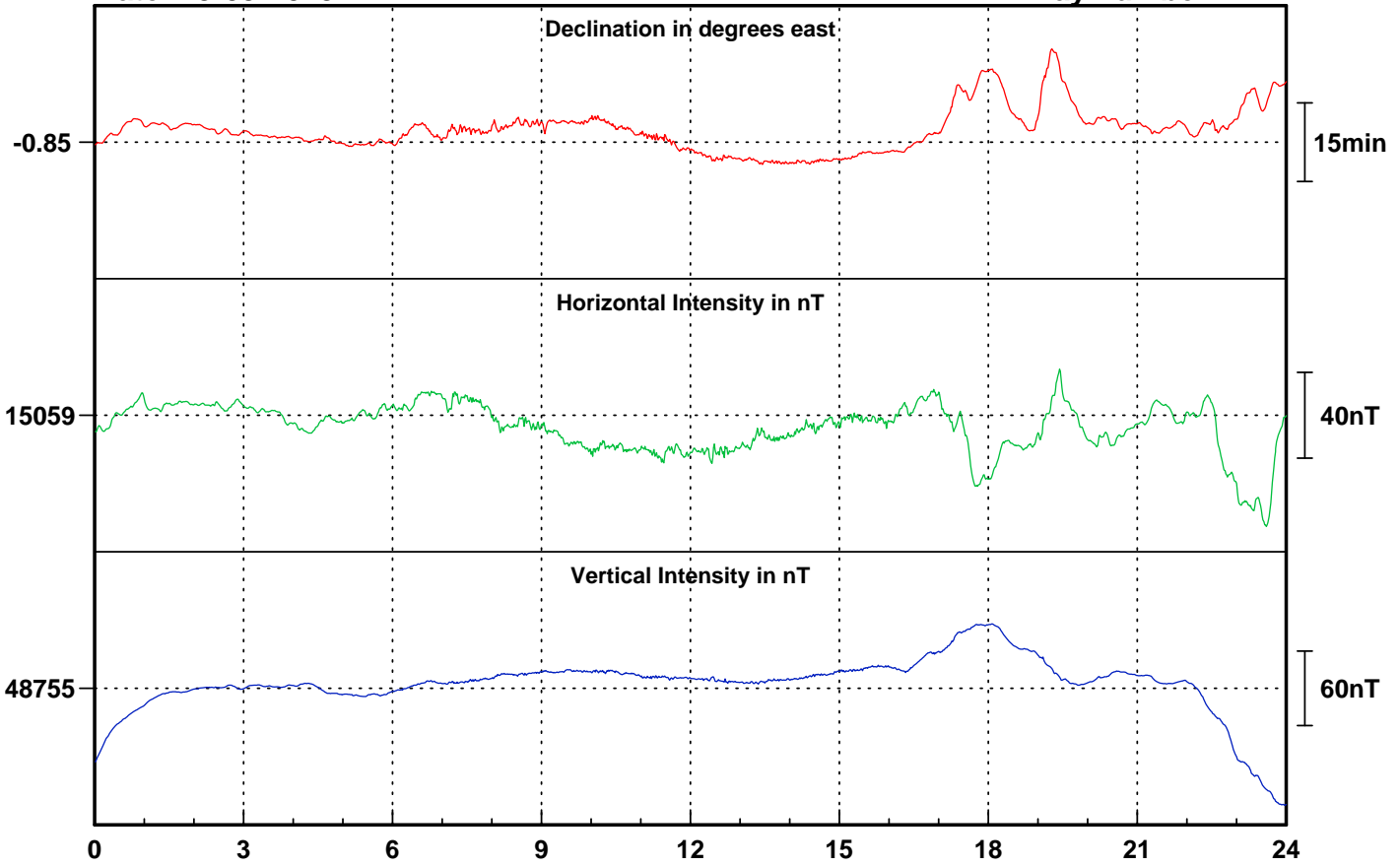
Day number: 271



Date: 29-09-2019

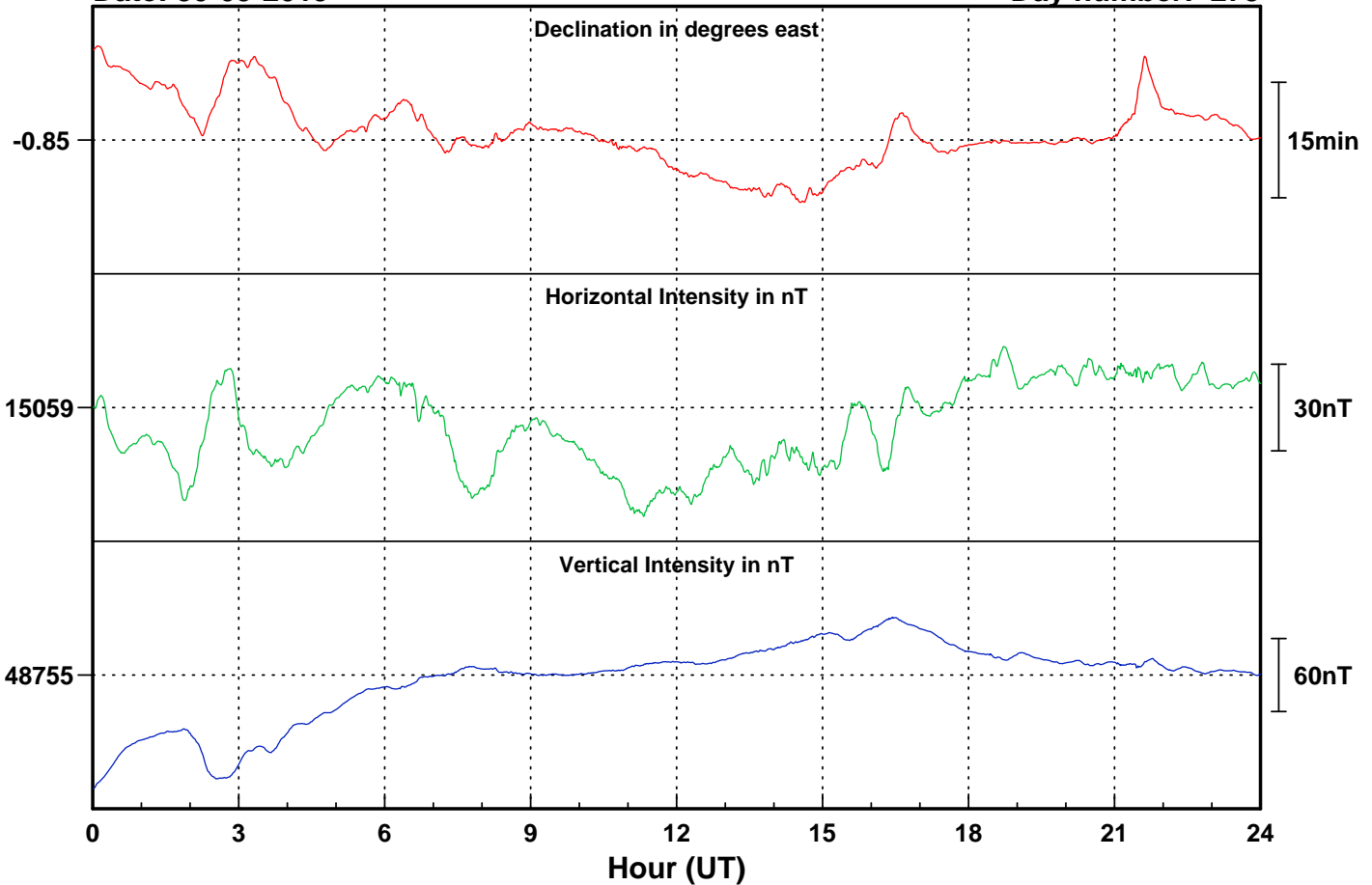
Lerwick

Day number: 272

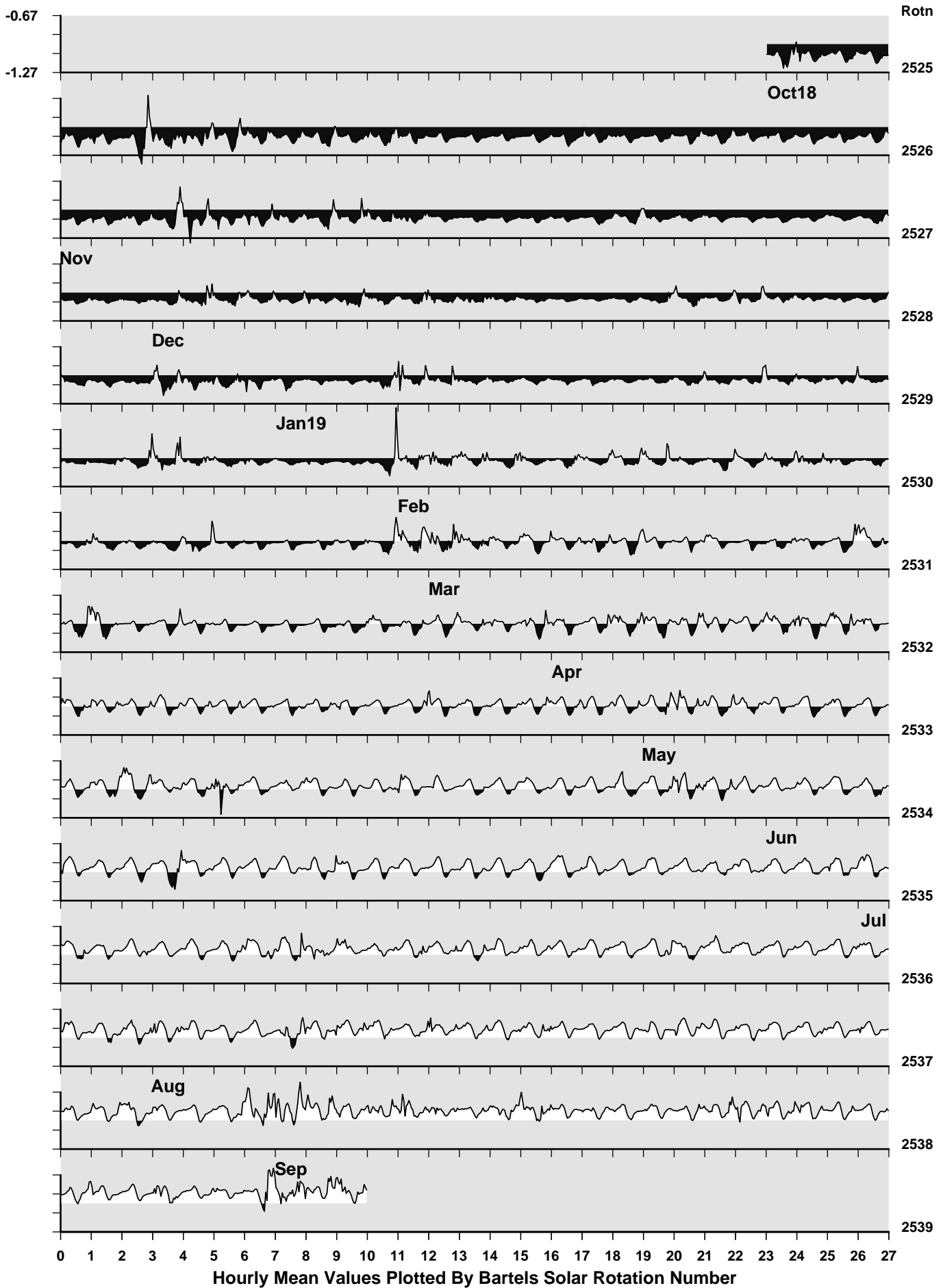


Date: 30-09-2019

Day number: 273

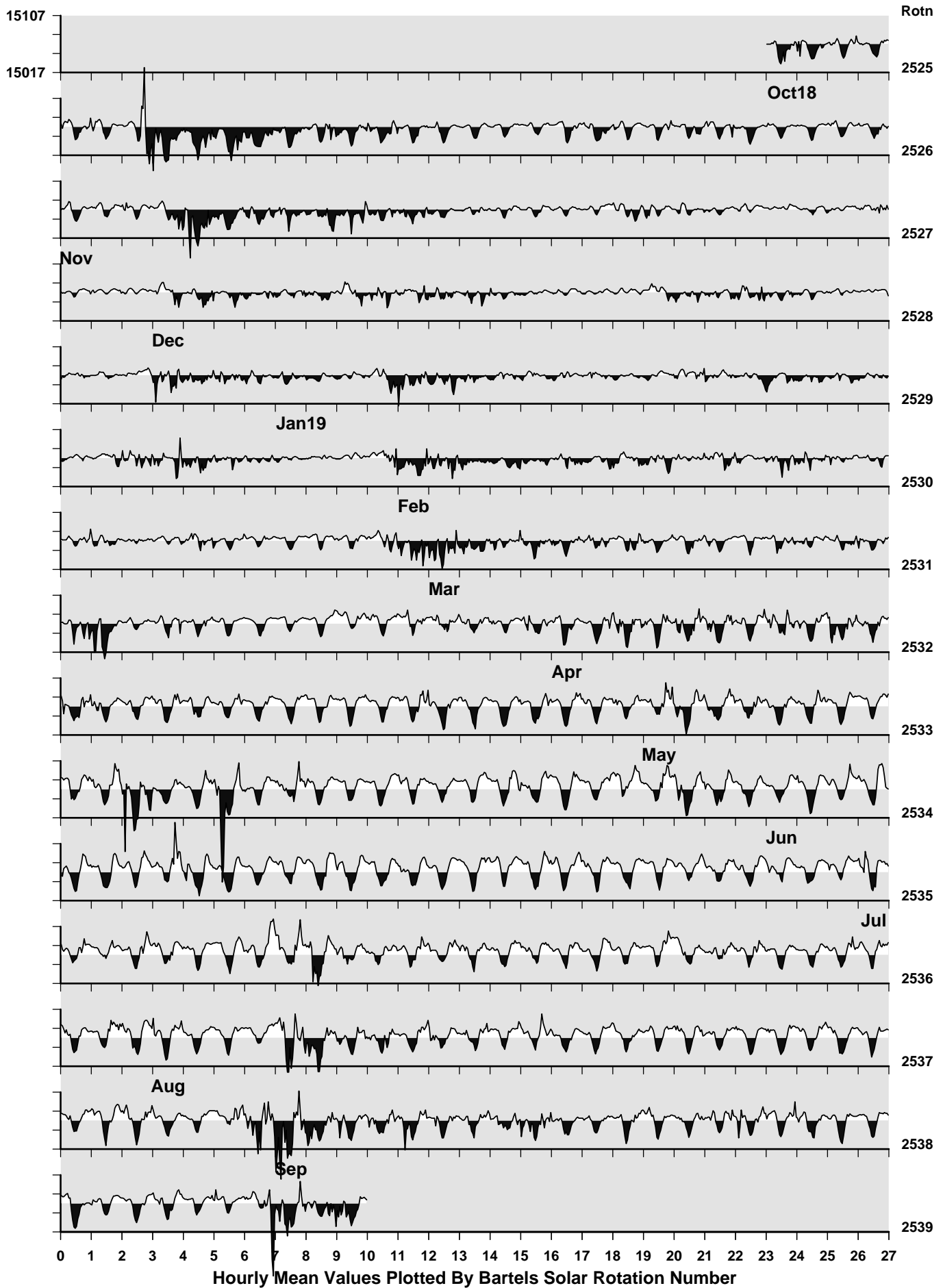


Lerwick Observatory: Declination (degrees)



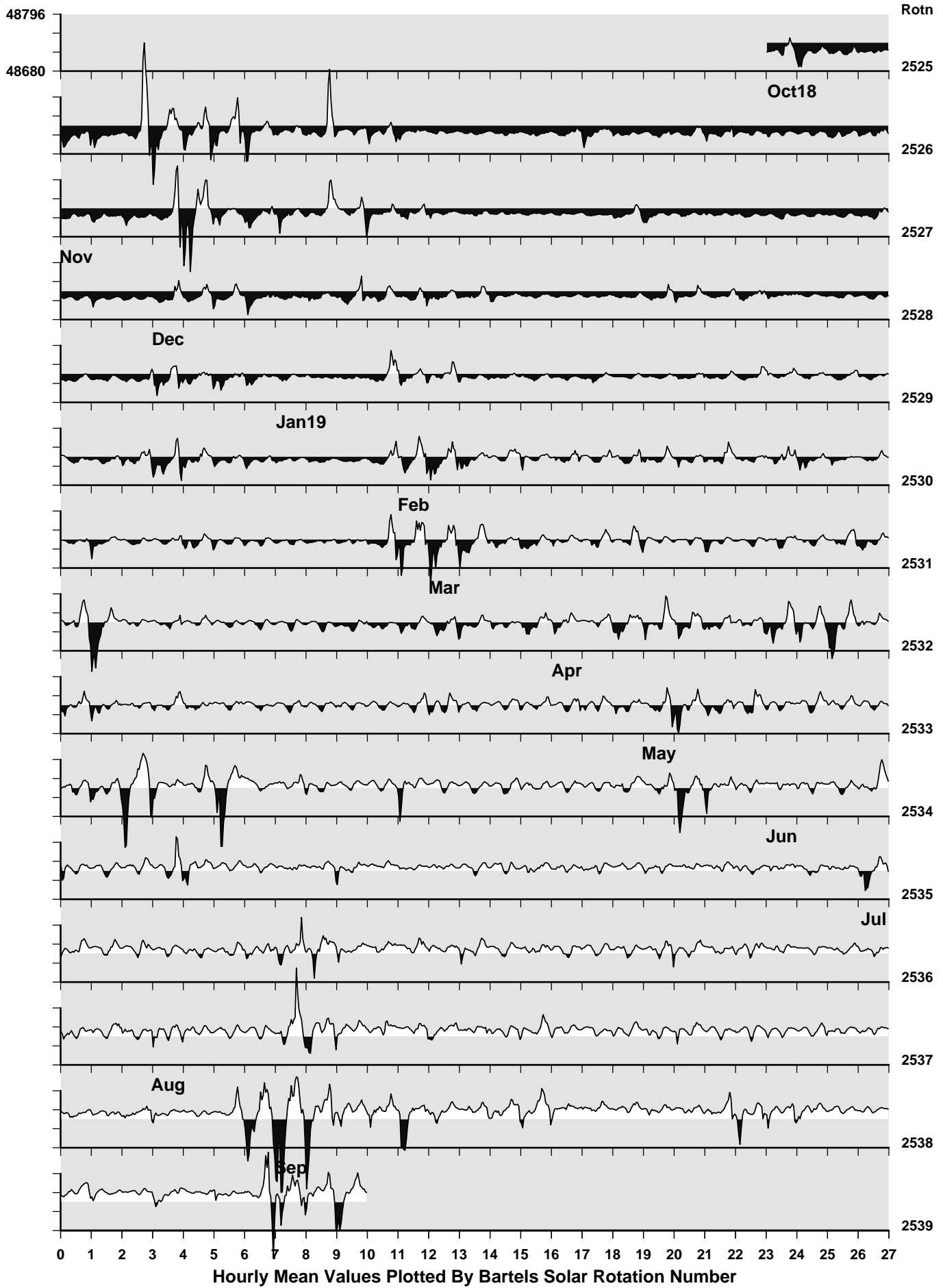
Hourly Mean Values Plotted By Bartels Solar Rotation Number

Lerwick Observatory: Horizontal Intensity (nT)



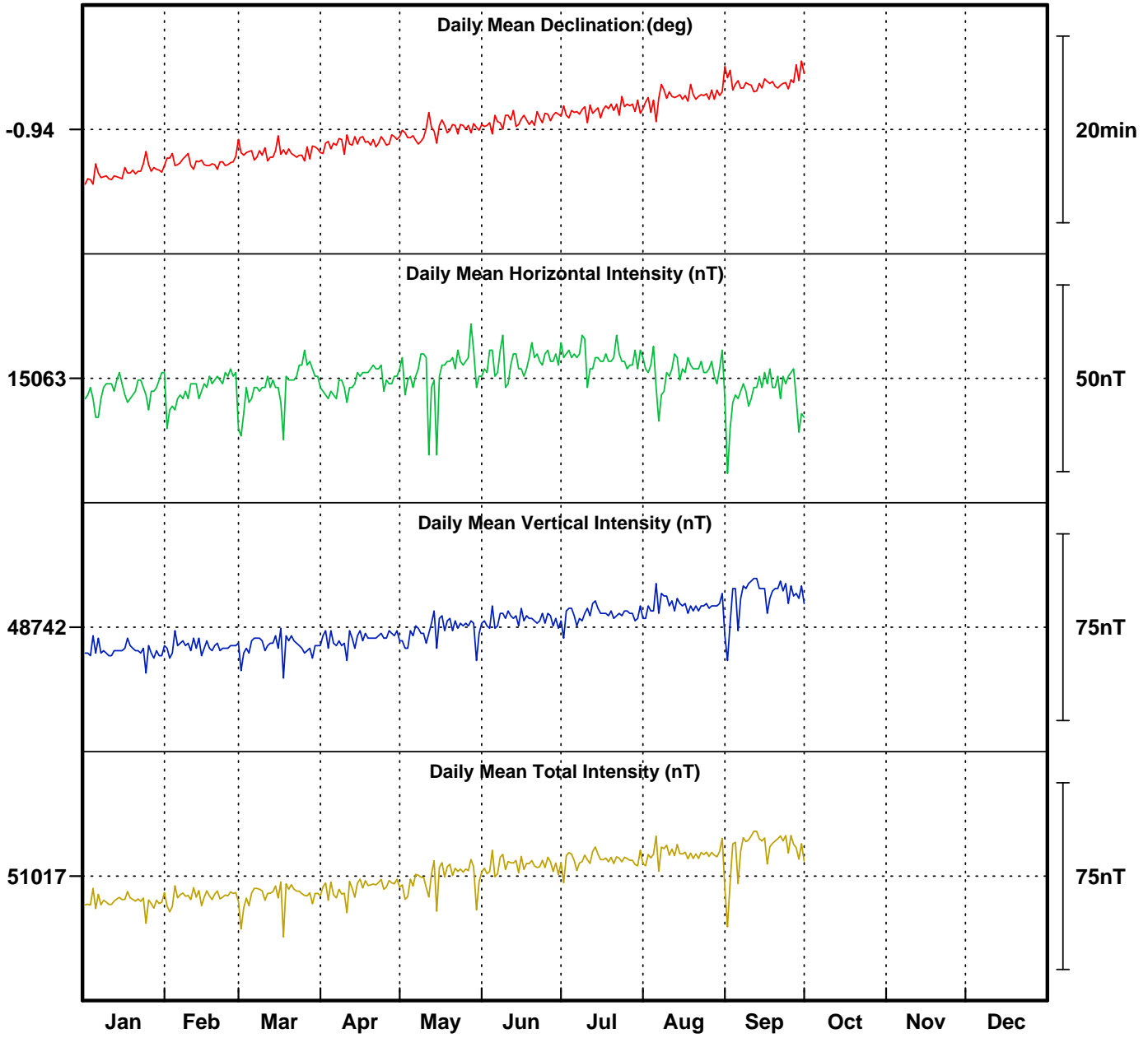
Hourly Mean Values Plotted By Bartels Solar Rotation Number

Lerwick Observatory: Vertical Intensity (nT)



Hourly Mean Values Plotted By Bartels Solar Rotation Number

Lerwick Observatory 2019



Monthly Mean Values for Lerwick Observatory 2019

| Month | <i>D</i> | <i>H</i> | <i>I</i> | <i>X</i> | <i>Y</i> | <i>Z</i> | <i>F</i> |
|-----------|-----------|----------|-----------|----------|----------|----------|----------|
| January | -1° 01.0′ | 15060 nT | 72° 49.6′ | 15058 nT | -267 nT | 48733 nT | 51007 nT |
| February | -0° 59.7′ | 15060 nT | 72° 49.6′ | 15058 nT | -262 nT | 48735 nT | 51009 nT |
| March | -0° 58.8′ | 15061 nT | 72° 49.6′ | 15059 nT | -258 nT | 48735 nT | 51009 nT |
| April | -0° 57.7′ | 15063 nT | 72° 49.6′ | 15060 nT | -253 nT | 48738 nT | 51012 nT |
| May | -0° 56.4′ | 15065 nT | 72° 49.5′ | 15063 nT | -247 nT | 48741 nT | 51016 nT |
| June | -0° 55.3′ | 15068 nT | 72° 49.4′ | 15066 nT | -242 nT | 48746 nT | 51021 nT |
| July | -0° 54.2′ | 15069 nT | 72° 49.3′ | 15067 nT | -237 nT | 48748 nT | 51024 nT |
| August | -0° 52.7′ | 15065 nT | 72° 49.7′ | 15063 nT | -231 nT | 48751 nT | 51026 nT |
| September | -0° 51.3′ | 15059 nT | 72° 50.1′ | 15058 nT | -225 nT | 48755 nT | 51028 nT |

Note

i. The values shown here are provisional.

LERWICK RAPID VARIATIONS

SI and SSCs

| Date | Time (UT) | Type | Quality | H (nT) | D (min) | Z (nT) |
|----------|-----------|------|---------|----------|---------|--------|
| 27-09-19 | 05 56 | SSC | B | 6.5/-7.8 | -2.27 | -2.8 |

Notes:

An asterisk (*) indicates that the principal impulse was preceded by a smaller reversed impulse.

The quality of the event is classified as follows:

A = very distinct

B = fair, ordinary, but unmistakable

C = doubtful

The amplitudes given are for the first chief movement of the event.

SFEs

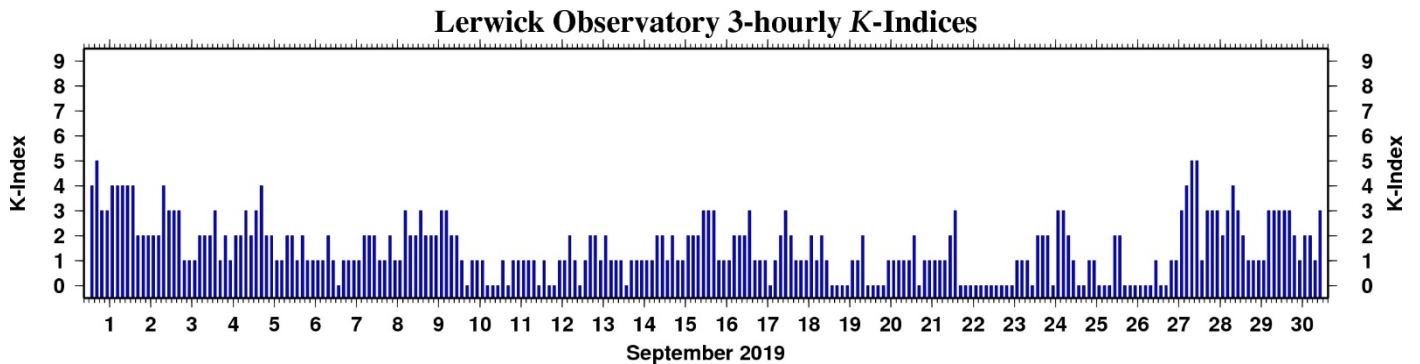
| Date | Universal Time | | | H (nT) | D (min) | Z (nT) |
|------|----------------|---------|-----|--------|---------|--------|
| | Start | Maximum | End | | | |
| None | | | | | | |

Note:

The amplitudes given are for the first chief movement of the event.

INDICES OF GEOMAGNETIC ACTIVITY

| Day | K - INDICES FOR THREE-HOUR INTERVAL | | | | | | | |
|-----|-------------------------------------|-------|-------|-------|-------|-------|-------|-------|
| | 00-03 | 03-06 | 06-09 | 09-12 | 12-15 | 15-18 | 18-21 | 21-24 |
| 1 | 4 | 5 | 3 | 3 | 4 | 4 | 4 | 4 |
| 2 | 4 | 2 | 2 | 2 | 2 | 2 | 4 | 3 |
| 3 | 3 | 3 | 1 | 1 | 1 | 2 | 2 | 2 |
| 4 | 3 | 1 | 2 | 1 | 2 | 2 | 3 | 2 |
| 5 | 3 | 4 | 2 | 2 | 1 | 1 | 2 | 2 |
| 6 | 1 | 2 | 1 | 1 | 1 | 1 | 2 | 1 |
| 7 | 0 | 1 | 1 | 1 | 1 | 2 | 2 | 2 |
| 8 | 1 | 1 | 2 | 1 | 1 | 3 | 2 | 2 |
| 9 | 3 | 2 | 2 | 2 | 3 | 3 | 2 | 2 |
| 10 | 1 | 0 | 1 | 1 | 1 | 0 | 0 | 0 |
| 11 | 1 | 0 | 1 | 1 | 1 | 1 | 1 | 0 |
| 12 | 1 | 0 | 0 | 1 | 1 | 2 | 1 | 0 |
| 13 | 1 | 2 | 2 | 1 | 2 | 1 | 1 | 1 |
| 14 | 0 | 1 | 1 | 1 | 1 | 1 | 2 | 2 |
| 15 | 1 | 2 | 1 | 1 | 2 | 2 | 2 | 3 |
| 16 | 3 | 3 | 1 | 1 | 1 | 2 | 2 | 2 |
| 17 | 3 | 1 | 1 | 1 | 0 | 1 | 2 | 3 |
| 18 | 2 | 1 | 1 | 1 | 2 | 1 | 2 | 1 |
| 19 | 0 | 0 | 0 | 0 | 1 | 1 | 2 | 0 |
| 20 | 0 | 0 | 0 | 1 | 1 | 1 | 1 | 1 |
| 21 | 2 | 0 | 1 | 1 | 1 | 1 | 1 | 2 |
| 22 | 3 | 0 | 0 | 0 | 0 | 0 | 0 | 0 |
| 23 | 0 | 0 | 0 | 0 | 1 | 1 | 1 | 0 |
| 24 | 2 | 2 | 2 | 0 | 3 | 3 | 2 | 1 |
| 25 | 0 | 0 | 1 | 1 | 0 | 0 | 0 | 2 |
| 26 | 2 | 0 | 0 | 0 | 0 | 0 | 0 | 1 |
| 27 | 0 | 0 | 1 | 1 | 3 | 4 | 5 | 5 |
| 28 | 1 | 3 | 3 | 3 | 2 | 3 | 4 | 3 |
| 29 | 2 | 1 | 1 | 1 | 1 | 3 | 3 | 3 |
| 30 | 3 | 3 | 2 | 1 | 2 | 2 | 1 | 3 |



The *aa* Index

| Date | Day | 3-hourly <i>aa</i> -indices | | | | | | | | <i>Aa_{am}</i> | <i>Aa_{pm}</i> | <i>Aa</i> |
|--------------------|-----|-----------------------------|----|-----|----|-----|----|----|----|------------------------|------------------------|-----------|
| 01-09-19 | 244 | 37 | 45 | 102 | 81 | 102 | 67 | 67 | 80 | 66.3 | 78.8 | 72.5 |
| 02-09-19 | 245 | 80 | 32 | 32 | 24 | 20 | 32 | 67 | 37 | 42.1 | 39.0 | 40.6 |
| 03-09-19 | 246 | 24 | 12 | 24 | 12 | 24 | 12 | 12 | 12 | 18.0 | 15.0 | 16.5 |
| 04-09-19 | 247 | 24 | 16 | 24 | 20 | 24 | 16 | 37 | 12 | 21.1 | 22.4 | 21.7 |
| 05-09-19 | 248 | 37 | 37 | 24 | 32 | 24 | 16 | 12 | 20 | 32.7 | 18.0 | 25.4 |
| 06-09-19 | 249 | 9 | 24 | 8 | 24 | 8 | 8 | 12 | 5 | 16.3 | 8.2 | 12.2 |
| 07-09-19 | 250 | 2 | 8 | 12 | 8 | 16 | 16 | 16 | 20 | 7.5 | 17.0 | 12.3 |
| 08-09-19 | 251 | 9 | 12 | 16 | 20 | 16 | 24 | 20 | 24 | 14.3 | 21.0 | 17.7 |
| 09-09-19 | 252 | 20 | 12 | 16 | 46 | 32 | 45 | 12 | 20 | 23.4 | 27.3 | 25.4 |
| 10-09-19 | 253 | 9 | 5 | 5 | 12 | 24 | 2 | 2 | 5 | 7.8 | 8.6 | 8.2 |
| 11-09-19 | 254 | 5 | 5 | 12 | 12 | 8 | 8 | 5 | 2 | 8.6 | 5.8 | 7.2 |
| 12-09-19 | 255 | 9 | 5 | 8 | 20 | 12 | 16 | 12 | 8 | 10.6 | 11.9 | 11.3 |
| 13-09-19 | 256 | 12 | 16 | 16 | 8 | 12 | 12 | 8 | 5 | 13.0 | 9.2 | 11.1 |
| 14-09-19 | 257 | 2 | 16 | 8 | 12 | 12 | 5 | 12 | 16 | 9.6 | 11.2 | 10.4 |
| 15-09-19 | 258 | 8 | 24 | 12 | 12 | 9 | 8 | 24 | 24 | 13.9 | 16.3 | 15.1 |
| 16-09-19 | 259 | 37 | 45 | 5 | 8 | 8 | 24 | 20 | 20 | 23.9 | 17.9 | 20.9 |
| 17-09-19 | 260 | 20 | 8 | 8 | 5 | 2 | 5 | 24 | 45 | 10.1 | 19.2 | 14.7 |
| 18-09-19 | 261 | 20 | 9 | 16 | 16 | 32 | 8 | 12 | 8 | 15.3 | 14.9 | 15.1 |
| 19-09-19 | 262 | 5 | 2 | 5 | 5 | 8 | 5 | 9 | 2 | 4.5 | 6.1 | 5.3 |
| 20-09-19 | 263 | 8 | 5 | 2 | 5 | 5 | 5 | 5 | 5 | 5.1 | 5.1 | 5.1 |
| 21-09-19 | 264 | 12 | 12 | 16 | 24 | 12 | 12 | 9 | 9 | 16.0 | 10.6 | 13.3 |
| 22-09-19 | 265 | 17 | 5 | 2 | 2 | 2 | 5 | 5 | 5 | 6.8 | 4.5 | 5.6 |
| 23-09-19 | 266 | 2 | 2 | 2 | 5 | 2 | 12 | 9 | 8 | 3.1 | 7.8 | 5.5 |
| 24-09-19 | 267 | 12 | 24 | 16 | 5 | 32 | 45 | 24 | 8 | 14.3 | 27.3 | 20.8 |
| 25-09-19 | 268 | 5 | 5 | 12 | 16 | 5 | 5 | 5 | 12 | 9.6 | 6.8 | 8.2 |
| 26-09-19 | 269 | 20 | 5 | 5 | 2 | 5 | 2 | 2 | 9 | 8.1 | 4.8 | 6.5 |
| 27-09-19 | 270 | 5 | 8 | 12 | 24 | 32 | 59 | 67 | 45 | 12.3 | 50.8 | 31.5 |
| 28-09-19 | 271 | 12 | 45 | 59 | 46 | 46 | 37 | 37 | 37 | 40.5 | 39.4 | 39.9 |
| 29-09-19 | 272 | 12 | 12 | 24 | 16 | 12 | 45 | 45 | 37 | 16.0 | 35.0 | 25.5 |
| 30-09-19 | 273 | 20 | 20 | 32 | 24 | 24 | 32 | 16 | 20 | 24.0 | 23.1 | 23.5 |
| Monthly Mean Value | | | | | | | | | | | 18.3 | |

Notes

- i. The units of the *aa* index are nT.
- ii. The 3-hour *aa* values are rounded to the nearest integer. Where $aa = *.5$, *aa* is rounded down.
- iii. Daily values (*Aa_{am}*, *Aa_{pm}* and *Aa*) are computed from *aa* values of original resolution.
- iv. The monthly mean value is computed from the daily mean values, *Aa*.
- v. Definitive *aa* indices are derived and published by the International Service for Geomagnetic Indices.

3-hourly *aa*-indices

